

## Research

# Projected changes in wet and dry extremes in the CMIP6 multi-model ensemble over the IGAD region of Eastern Africa

Paulino Omoj Omay<sup>1,2</sup> · Nzioka J. Muthama<sup>1</sup> · Christopher Oludhe<sup>1</sup> · Josiah M. Kinama<sup>1</sup> · Guleid Artan<sup>2</sup> · Zachary Atheru<sup>2</sup>

Received: 15 March 2024 / Accepted: 18 September 2024

Published online: 27 September 2024

© The Author(s) 2024 [OPEN](#)

## Abstract

Wet and dry days, as well as wet and dry spells, are crucial pieces of information for rain-fed agriculture, food security, and numerous socioeconomic activities in East Africa. This study examines the projected changes in wet/dry days and wet/dry spells using data from the Multi-Model Ensemble (MME) participating in the Coupled Model Intercomparison Project Phase 6 (CMIP6). Statistical criteria and thresholds are used to project the changes in wet and dry days, as well as wet and dry spells, under the shared socioeconomic pathways (SSP) scenarios (SSP1-2.6, SSP2-4.5, and SSP5-8.5) for the annual, March–May (MAM), June–September (JJAS), and October–December (OND) seasons. The analysis indicates that the CMIP6 models generally overestimate the number of wet days (wet spells) across all seasons and scenarios at the 1 mm threshold. A projected 10–20% increase in total rainfall over the IGAD region is driven by an increase in rainfall intensity and the number of wet days under all scenarios during the near (2021–2050) and far (2071–2100) futures. A decrease in wet days and spells (increase in dry days and spells) is projected over South Sudan in JJAS, while an increase in wet spells is projected over Kenya, Somalia, and Sudan in OND during the near and far future compared to the baseline period. By the end of the century, wet days are projected to increase by approximately 20–30%, and dry spells are projected to decrease by 10–20% under the SSP1-2.6 and SSP5–8.5 scenarios. The EnsMean 10 CMIP6 tends to smooth out the extremes (wet or dry biases), creating a result that may appear more accurate but does not reflect the extremes or variations projected by individual models over South Sudan, Uganda, Kenya and Ethiopia. The projected patterns of wet and dry spells under SSP1-2.6 highlight the importance of mitigation efforts to limit temperature rise to below 1.5°. It is necessary to model how shifts in extreme dry and wet conditions will likely affect climate-sensitive sectors, such as agriculture and food security, in order to make well-informed decisions.

**Keywords** CMIP6 · Projections · Eastern Africa · Wet days · Dry days · Wet spells · Dry spells · IGAD

## 1 Introduction

Climate changes and variability pose numerous hazards to socio-economic activities in East Africa [1]. According to the [2], the main drivers of climate change and Global Warming (GW) are anthropogenic activity and natural processes. The interplay between components of climate systems is complex [3]. Therefore, accurately measuring and projecting climate trends using General Circulation Models (GCMs), Regional Climate Models (RCMs), or downscaled products is crucial for the scientific community [4]. The temporal and spatial fluctuations in daily rainfall attributes

---

✉ Paulino Omoj Omay, paulinoomay@gmail.com | <sup>1</sup>Department of Earth and Climate Sciences, Faculty of Science & Technology, University of Nairobi, Nairobi, Kenya. <sup>2</sup>IGAD Climate Prediction and Application Centre (ICPAC), Nairobi, Kenya.



across East Africa are influenced by the complex terrain, as well as local and global factors [5, 6]. Multiple studies conducted in the region have shown that the March–April–May (MAM) and June–July–August–September (JJAS) seasons are inadequately simulated by the majority of GCMs and RCMs, compared to the October–November–December (OND) season. The frequency and intensity of droughts in the twentieth and twenty-first centuries have been exacerbated by year-to-year fluctuations in rainfall [7–10]. Furthermore, these droughts have been intensified by delayed onset of the rainy season, which ends earlier than usual and lasts for a shorter period of time [11].

Climate change is projected to intensify the frequency of as well as wet and dry spells. This can lead to a decrease in agricultural yields due to water-related stress [12, 13]. Wet and dry days, as well as wet and dry spells, refer to consecutive days with or without rain, with a threshold of 1 mm. These periods can last from a few weeks to several months, and if they continue for a long time, they can result in meteorological droughts or floods, which can have significant impacts on agriculture, water supply, and the environment [14]. The timing and duration of rainy days and dry spells are crucial for rain-fed agriculture and food security [15]. These changes are caused by more intense daily rainfall and a decrease in the number of days with rainfall [16]. As a result of water scarcity caused by these changes, food production and availability are reduced [17]. Intense rainfall events also affect the hydrological cycle by increasing runoff and soil saturation [17].

Climate models, such as the Coupled Model Intercomparison Project, Phase 5 (CMIP5) [18] and CMIP6 [19], provide insights into the historical and future characteristics of wet and dry days and spells. Studies utilizing these models have revealed variations in wet and dry signals across different regions in the tropics [20]. For example [21], found a decline in consecutive wet days in CMIP5 over the Greater Horn of Africa at global warming levels of 1.5 °C and 2 °C, while [22] reported an increase in the number of dry days and a decrease in the number of wet days over East Africa [20]. Also indicated that fewer rainy days and longer dry periods based on CMIP5 and CMIP6 simulations could expand arid climatic zones. CMIP6 is also used to investigate extreme events such as extreme precipitation events [23] and prolonged droughts, as well as assess the impact of these extremes on various sectors [24]. Model evaluation within CMIP6 involves comparing different climate models to understand variability and uncertainty, as well as identifying strengths and weaknesses in simulating wet and dry spells [25, 26]. Additionally, certain CMIP6 models are used to investigate atmospheric and oceanic conditions that influence wet and dry spells, as well as the role of large-scale climate phenomena such as El Niño–Southern Oscillation (ENSO) [27]. Many CMIP6 models project an increase in the frequency and intensity of both wet and dry spells due to climate change [28]. However, changes in wet and dry spells vary greatly by region, with some areas experiencing more significant changes than others [29, 30]. The variability among CMIP6 simulations and projections is considerable, highlighting the importance of using multiple models to understand the range of possible outcomes [31].

Although several studies have used CMIP6 simulations and projections to examine current and future climate trends in East Africa, there is a knowledge gap regarding the projected number of wet days, wet spells, dry days and dry spells. Most research in the region has focused on extreme events, using indices established by the Expert Team on Climate Change Detection Indices (ETCCDI), which are widely used in the region and other areas. Notable studies on extreme events in East Africa include [32] and [20], which focus on the characteristics of wet and dry seasons. Additionally [10], study rainfall variability, [33] examine drought patterns [6], investigate the rainfall annual cycle, and [22] compare earlier CMIPs products with CMIP6. All these studies have shown changes and variability in the patterns of extreme rainfall events in the CMIP5 and CMIP6 over the East Africa region.

Most of the studies mentioned above focused on total rainfall, wet and dry spells on an annual basis. However, to our knowledge, no study has described the projected changes in annual and seasonal rainfall totals, rainfall intensity, wet/dry days, and wet/dry spells over the IGAD region. The present study aims to fill this gap by analyzing the latest dataset from CMIP6 model simulations and projections over the IGAD region. Furthermore, to the best of our knowledge, no study has analyzed the CMIP6 datasets to examine the percentage of change (%) in annual and seasonal rainfall totals, rainfall intensity, wet/dry days, and wet/dry spells over the IGAD region in the twenty-first century using the Shared Socio-Economic Pathways (SSP1–2.6, SSP2–4.5, and SSP5–8.5). This information will be vital for decision-makers and policymakers in promoting sustainable regional development through effective adaptation and mitigation approaches that enhance the resilience of communities and key socioeconomic sectors in the IGAD region. The paper is organized as follows: Sect. 2 provides comprehensive information on the datasets and methodologies used, Sect. 3 presents the analysis findings, Sect. 4 offers a detailed discussion of the results, and Sect. 5 focuses on the summary and conclusion.

## 2 Data and methods

### 2.1 Data

#### 2.1.1 CMIP6 historical simulations and projection

This study used daily CMIP6 historical simulations and future projection scenarios for precipitation (referred to as rainfall in this study) from 1981 to 2014 for temporal analysis (timeseries), and 1985–2014 used as baseline and 2015–2100 (future scenarios), which divided into near future (2021–205) and far future (2071–2100). The projected shifts in wet/dry days and wet/dry spells were assessed using the Shared Socio-Economic Pathways (SSP) under SSP1-2.6, SSP2-4.5 and SSP5-8.5 as low, medium and business as usual emission scenarios. The SSP1-2.6 scenario represents a gradual transition towards global sustainability. The SSP2-2.5 scenario, on the other hand, does not include significant changes compared to the baseline period. Lastly, the SSP5-8.5 scenario assumes no significant climate change legislation, with everything operating as normal. The data utilized in this study were acquired from the CMIP6 website (<https://esgf-node.llnl.gov/search/cmip6/>). We specifically used the first member realization outputs (r1i1p1f1) from a variety of models in CMIP6 to ensure inter-comparison and consistency. The datasets used in this study include 23 models as well as Multi-Model Ensemble (MME or EnsMean) data from the top 10 CMIP6 models that performed the best. These models were selected based on their performance over the IGAD region of eastern Africa [34]. The full list of 23 CMIP6, validation processes, institution, country, and geographic resolution associated with each model found in study by [35]. The list of 10 CMIP6 models that performed the best and used in computing MME or EnsMean and patterns of projected changes in wet/dry days, wet/dry spells presented in Table 1.

#### 2.1.2 CHIRPS v2.0 datasets

The Climate Hazards Group (CHG) Infrared Precipitation with in-situ station (CHIRPS v2.0) [36] daily records from 1981 to 2014 for temporal analysis (timeseries), and 30 year period (1985–2014) used as baseline recommended by the World Meteorological Organization (WMO). CHIRPS v2.0 was chosen as the reference data because it outperformed other Satellite-based rainfall estimates (SRE) datasets in the IGAD region, as demonstrated by studies conducted by [37–40], and [41]. The CHIRPS product was developed with a spatial resolution of 0.05°, providing data at daily, pentadal, dekadal, and monthly time intervals. The data is freely accessible from the University of California at Santa Barbara (UCSB) portal for the historical and present (1981 to the present). The data has been validated and used by other researchers in the region in previous studies [37, 41–43]. To address the issues related to the resolution discrepancies between the CMIP6 models and CHIRPS, a total of 23 models and CHIRPS datasets were adjusted by scaling down their resolutions to a uniform ten-kilometer (0.1 deg) scale customized for IGAD region (Fig. 1). This rescaling process was carried out using the remapbil interpolation technique, uses bilinear interpolation for remapping (transforming) images or pixels [44]. Noting that remapbil interpolation has limitations compared to remapcon interpolation when used for conservative variables, such as precipitation. Remapcon interpolation works well for non-conservative variables, like temperature [68].

**Table 1** List of the top ten CMIP6 performances over the IGAD region that were used to calculate the Multi-Model Ensemble (EnsMean), together with the names, institutions, and spatial resolutions of the models

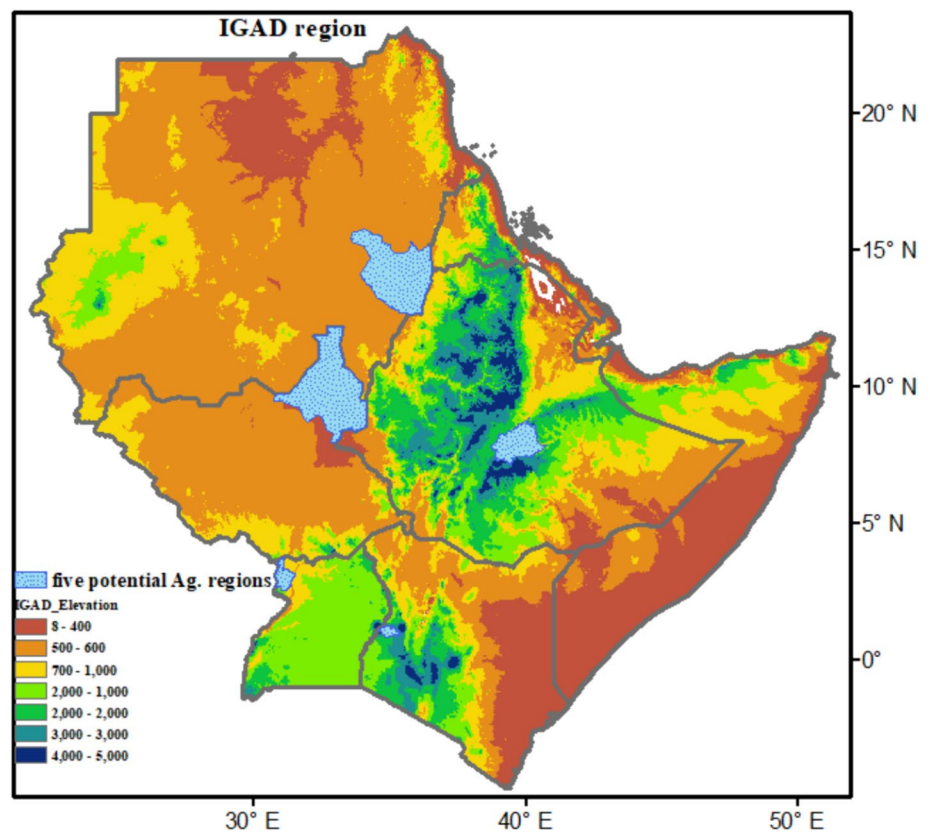
	CMIP6 Model Name	Institution	Country	Coarse resolution
1	BCC-CSM2-MR	BBC	China	1.1° × 1.1°
2	CMCC-CM2-HR4	CMCC	Italy	0.942° × 1.25°
3	EC-Earth3	EC-Earth Consortium	Europe	0.7° × 0.7°
4	GFDL-ESM4	NOAA-GFDL	USA	1.3° × 1°
5	HadGEM3-GC31-MM	MOHC	UK	0.942° × 1.25°
6	INM-CM5-0	INM	Russia	2° × 1.5°
7	IPSL-CM6A-LR	IPSL	France	2.5° × 1.3°
8	MIROC6	JAMSTEC	Japan	1.4° × 1.4°
9	NorESM2-MM	NCC	Norway	0.94° × 1.25°
10	TaiESM1	CliCS	Taiwan	1.25° × 0.94°

## 2.2 Methods

### 2.2.1 Criterion and threshold for rainfall intensity, wet days and dry spells

This study examined projected changes in wet/dry days and wet/dry spells using well-defined criteria and thresholds. The daily rainfall measurement of 1 mm, which used by [45] for dry days adopted as the threshold to identify wet or dry days. The term "number of wet days" typically refers to the count of days with at least a 1 mm threshold (above 1 mm), while the term "number of dry days" refers to the count of days without at least 1 mm (below 1 mm). The term "number of wet spells" refers to the count of distinct periods with 7 consecutive days with at least 1 mm, while the term "number of dry spells" refers to the count of distinct periods without 7 consecutive days with at least 1 mm. The 7 consecutive days with rain (without rain) is the threshold for wet spells (dry spells). In other words, the consecutive 7, 14, 21, and 28 days translated to 1, 2, 3, and 4 spells, respectively. An increase or decrease in wet days does not necessarily lead to an increase or decrease in dry spells, and an increase or decrease in dry spells is not necessarily associated with an increase or decrease in wet spells. Therefore, this study focuses on patterns of wet days, wet spells, dry days, and dry spells instead of just wet days and dry days or wet spells and dry spells. In addition, while 1 mm threshold used to compute rainfall intensity. The adoption of the 1 mm threshold is supported by the recommendation of the Expert Team on Climate Change Detection and Indices (ETCCDI) [46] for assessing extreme rainfall events. Several studies worldwide have also used the 1 mm threshold for various purposes, such as computing wet days and dry spells in Equatorial Eastern Africa [47], determining drought and flood thresholds [48], analyzing day days [49], simulating and projecting wet and dry spells in models [20, 50, 51], and studying onset and cessation [11]. These criteria and thresholds are particularly suitable for ensuring reliable and accurate food crop production, as food crops are crucial for food availability and security. The annual number of possible wet/dry days is 365/366 days (52 spells), while the seasonal number ranges from 90 to 91 days (13 spells) for DJF to 92 days (13 spells) for MAM and OND, and 122 days (17 spells) for JJAS season.

**Fig. 1** Topographic map showing the altitude variations within the IGAD region of Eastern Africa. The sky-blue areas that have the potential to be used for agricultural purposes used in temporal analysis. The digital elevation model (DEM) datasets were retrieved from shuttle radar topography Mission (SRTM) 90 m spatial resolution <http://dds.cr.usgs.gov/srtm/>



## 2.2.2 Statistical methods for wet/dry days and wet/dry spells

The simple arithmetic mean (SAM) and summation is used to calculate the Multi-model Mean Ensemble (MME or EnsMean), and total rainfall. SAM is utilized to minimize the model uncertainties [52] and to overestimate/underestimate observed climate patterns. Several studies have employed this method to compute the MME of model simulations [53, 54]. The SAM time series is derived from an ensemble of the top 10 best-performing CMIP6 historical simulations. In this study, SAM is generated by simply averaging the top ten best-performing CMIP6 GCMs historical simulations using Eq. 1. Due to inconsistencies in the CMIP6 model, the patterns of changes in wet/dry days and wet/dry spells were computed separately for each of the 10 models before taking the ensemble, in order to avoid or reduce inconsistencies in the CMIP6. The full list of 23 CMIP6 institutions, countries, and geographic resolutions associated with each model, as well as the validation processes, and how the 10 best performance models used in this study were selected, can be found in the study by Omay et al. [36].

$$SAM^- = \frac{1}{N} \sum_{i=1}^n CMIP6_i \quad (1)$$

$N$  is the total number of CMIP6 GCMs used in historical simulations, with  $n$  representing the 10 models listed in Table 1 above. The complete validation results and statistical indices used to select these 10 models can be found in [34]. Additionally, the SAM was utilized to compute the spatial mean patterns of wet and dry days, as well as wet and dry periods, for the near future (2021–2050) and the far future (2071–2100), in comparison to the reference period of 1985–2014 (baseline). The near and far future spatial means of wet and dry days, wet and dry spells, under SSP1-2.6, SSP2-4.5, and SSP5-8.5, were then subtracted from the baseline, as described in Eq. 2 below. This process provides a comprehensive understanding of the future changes relative to the baseline period.

$$\nabla \bar{X} = \frac{1}{N} \left( \sum_{j=1}^n X_j \right) - \frac{1}{N} \left( \sum_{i=1}^n X_i \right) \quad (2)$$

where,  $(X_j)$  represents the near future (2021–2050) and far future (2051–2080), and  $(X_i)$  represents the baseline period (1981–2000) for wet/dry days and wet/dry spells. The magnitude of change in percentage (%) is then determined using Equation 3.

$$\text{Rate of change}(\nabla X\%) = \left( \frac{\nabla X}{X_i} \right) * 100 \quad (3)$$

The time series analysis (temporal analysis) of wet and dry days, as well as wet and dry spells, was computed for the El Gadaref state of Sudan, the Upper Nile state of South Sudan, the Arsi zone of Ethiopia, the Trans Nzoia County of Kenya, and the Arua district of Uganda. These sub-regions were selected based on their potential as the top five food baskets in the IGAD region. The extracted time series were used to illustrate the yearly cycle of wet days, demonstrating the level of agreement between the reference data (CHIRPS) and CMIP6 models. Boxplots, also known as box-and-whisker plots, were used to evaluate the fluctuations and differences in wet and dry days, as well as wet and dry spell patterns, under low and high emission scenarios (specifically SSP1-2.4 and SSP5-8.5). Python, Climate Data Operators (CDO), Climate Data Tool (CDT) [55], and ArcGIS 10.4 were the tools employed for displaying spatial and temporal patterns.

## 3 Results and discussions

### 3.1 Wet days and dry spells over the reference period (1985–2014)

Figures 2 and 3 show the average number of wet days and dry spells across the IGAD region during the reference period (1985–2014). These results are based on historical simulations of each of the 23 CMIP6 models. The figures include the ensemble mean (EnsMean) of these 23 models, as well as the ensemble mean of the top 10 performing models. The findings indicate that the highest number of wet days was simulated in various regions, including South Sudan, central, western, and northern Ethiopia, as well as central and northern Uganda. With the exception of

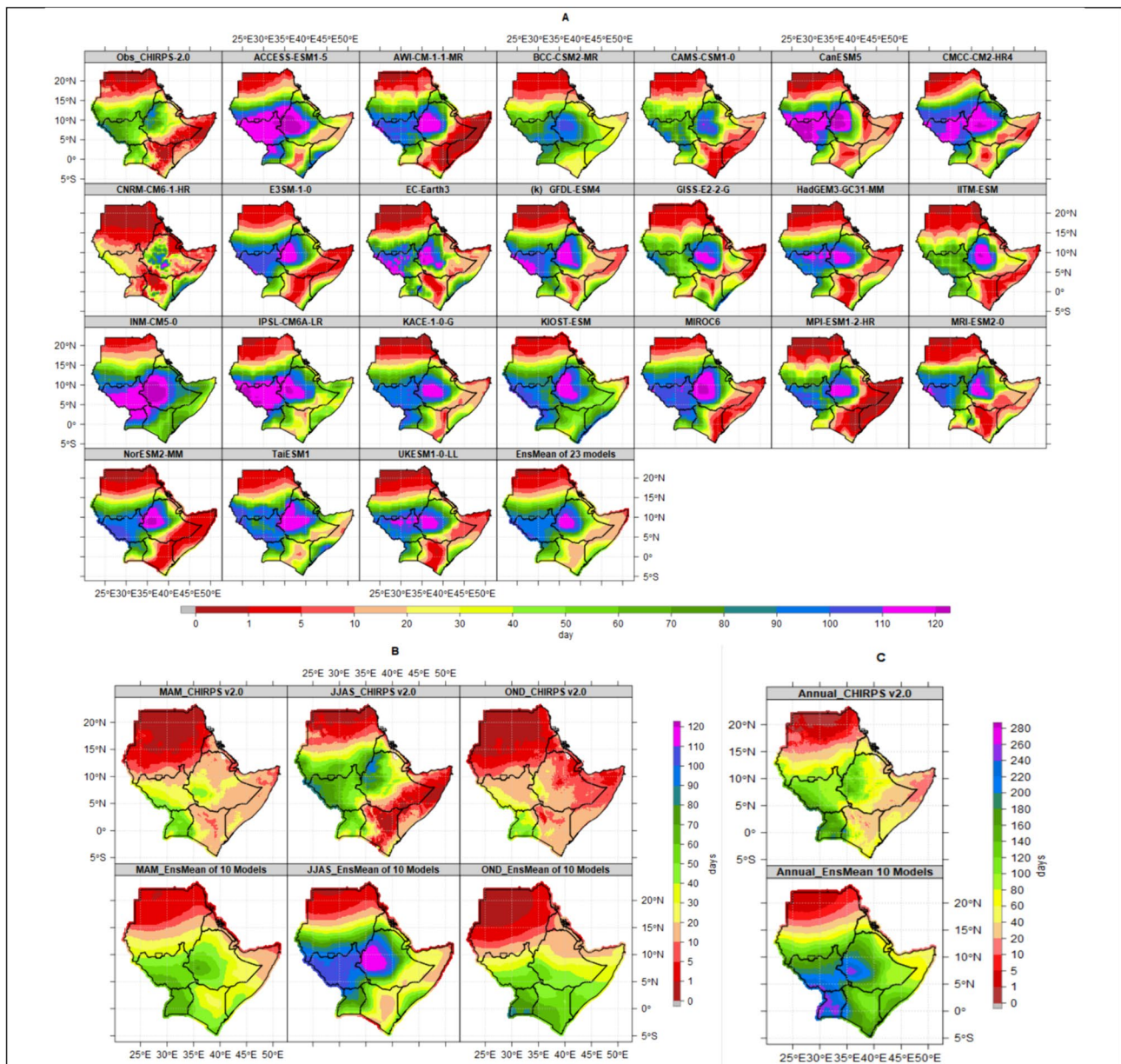


**Fig. 2** Spatial patterns of seasonal and annual wet days simulated by 23 CMIP6 historical run and ensemble mean (EnsMean) during JJAS season (A), EnsMean of 10 best performances during MAM, JJAS and OND seasons (B) and annual time-scale (C) relative to CHIRPS v2.0 reference datasets and 1985–2014 baseline

CNRM-CM6-1-HR, all the other CMIP6 models analyzed in this study tended to overestimate the number of rainy days at the 1 mm threshold. During the JJAS period, models such as ACCESS-ESM1-5, CanESM5, INM-CM5-0, IPSL-CM6A-LR, MIROC6, and NorESM2-MM simulated between 110 and 122 wet days in the highlands of western Ethiopia, out of a total of 122 possible wet days, while the highest number of wet days based on CHIRPS v2.0 reference data did not exceed 90 days (Fig. 2b). On the annual timescale, the number of wet days recorded in the central and southern sections of South Sudan, Uganda, and western Ethiopia ranged from 120 to 180 days based on CHIRPS v2.0 reference data. However, the CMIP6 EnsMean model simulated a higher number of wet days, ranging from 200 to 250 days. This indicates an overestimation of the occurrence of wet days when considering a threshold of 1 mm (Fig. 2C). The arid and semi-arid areas in eastern and northern Kenya, districts in southern and central Somalia, zones in the southeastern sections of Ethiopia, as well as northern provinces in Sudan, experienced the fewest days of rainfall throughout all seasons. The progression of wet days in the MAM, JJAS, and OND seasons consistently corresponds with the wet and

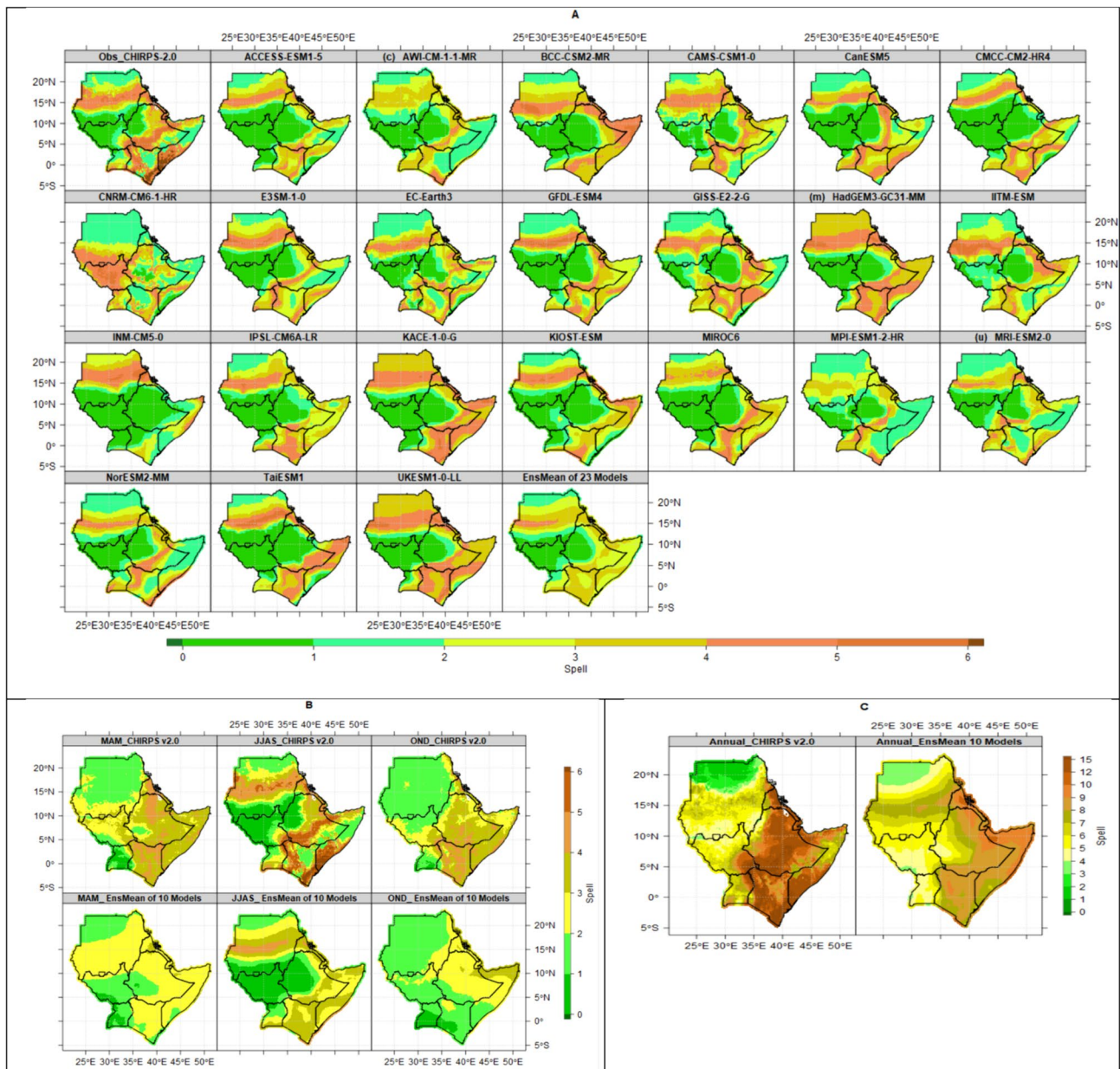


**Fig. 3** Spatial patterns of seasonal and annual dry spells simulated by 23 CMIP6 historical run and ensemble mean (EnsMean) during JJAS season **(A)**, EnsMean of 10 best performances during MAM, JJAS and OND seasons **(B)** and annual time-scale **(C)** relative to CHIRPS v2.0 reference datasets and 1985–2014 baseline

dry seasons in most parts of the East Africa region [20]. Furthermore, the majority of models inaccurately simulated higher levels of wet days in the coastal regions of Kenya. The average of the top 10 performing models aligns more closely with CHIRPS v2.0 than the average of all 23 models. These findings are consistent with [56] results, which showed that the ensemble of models generally provides a more accurate representation of precipitation and associated extremes compared to individual models. The simulated patterns of wet days in the CMIP6 models reveal the primary cause for the overestimated spatial distribution of rainfall totals throughout most of the IGAD region [35]. The variation in the number of wet days per season is influenced by different climate systems, such as the Arabian Peninsula climate system, which brings deeper monsoons and low-level cyclonic flow. This is particularly evident during the JJAS season in the northern sector of Eastern Africa, where convective moisture systems are transported and intensified [57, 58].

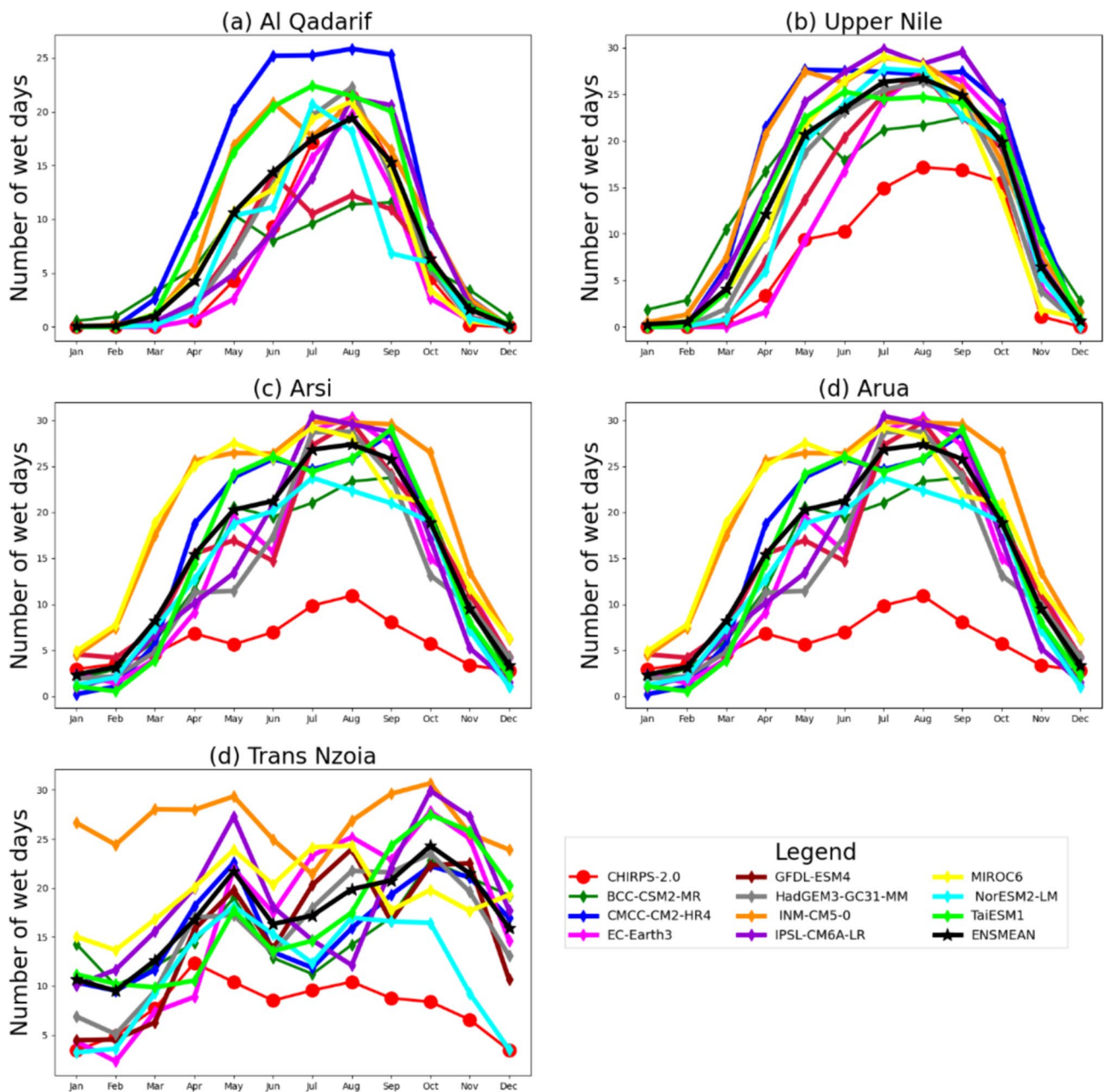
Figure 3 demonstrates the ability of the 10 CMIP6 models and ensemble mean to accurately replicate the average minimum and maximum duration of dry spells in the IGAD region. According to most models, it is stimulated that the majority of counties in South Sudan, zones in western Ethiopia, and districts in central and northern Uganda will experience a maximum of one dry spell period (7 consecutive wet days). In the western and southwestern regions of South Sudan, most zones in western Ethiopia, and districts in northern Uganda, there will not be a continuous 7-day period without rainfall, with a minimum threshold of 1 mm. The JJAS season, which represents the primary rainy season in most areas of the IGAD region, has shorter periods of dry spells compared to the MAM and OND seasons. On the other hand, Kenya, Somalia, and southeastern Ethiopia have the longest periods of dry spells, while southwestern South Sudan, western Ethiopia, and central and northern Uganda have the shortest. It is worth noting that the CNRM-CM6-1-HR model indicates a higher occurrence of prolonged dry spells across most of Sudan. In terms of accuracy, dry spells were overestimated by 23 CMIP6 models and EnsMean during the JJAS season (Fig. 3A), EnsMean of the top 10 performances during the MAM, JJAS, and OND seasons (Fig. 3B), and on an annual time-scale (Fig. 3C) in comparison to CHIRPS v2.0. Generally, the IGAD region does not experience dry spells lasting more than 5 consecutive periods without rainfall. The regions with the longest periods of consecutive dry spells also exhibit a notable increase in rainfall variability according to the CMIP6 historical simulations [59].

Figure 4 presents the average monthly count of the number of wet days in five key rain-fed agriculture regions of Sudan, South Sudan, Ethiopia, Kenya, and Uganda. These regions play a crucial role in food production within the IGAD region. The purpose of conducting a monthly count of rainy days was to evaluate the accuracy and reliability of using a 1 mm threshold for rain gauge, satellite rainfall estimates, model simulations, and projection applications. The use of the 1 mm threshold recommended by ETCCDI [46] is to measure changes in extreme rainfall events, such as consecutive wet and dry days, wet and dry spells, and the identification of wet and dry seasons in CMIP5 and CMIP6 simulations [20]. All 10 models and EnsMean overestimated the number of wet days from January to December. This shows that the 1 mm threshold is not sufficient for accurately determining the number of rainy days (wet spells) due to the tendency of most models to overestimate such occurrences. All models consistently simulated that Arsi in Ethiopia and Arua in Uganda would receive rainfall every day in the months of June, July, August, and September. When compared to the CHIRPS v2.0 reference datasets, there was an average increase of 12–15 days was recorded as rainy days. This indicates that the majority of the 10 CMIP6 simulated extra 10–14 days compared to CHIRPS v2.0 during the peak of the rainy season from June to September. The patterns of the monthly cycle of the number of wet days from January to December were confirmed to be consistent with the study by [10], which demonstrated the ability of the CMIP6 model to duplicate the bimodal and unimodal rainfall patterns in East Africa. This is evidenced by the role played by the monthly distribution of wet day cycles in shaping the seasonal and annual total rainfall. Specifically, while the CHIRPS v2.0 average for wet days ranged from 12 to 15 days, the CMIP6 models simulated a range of 25–30 days. Therefore, using a rainy-day criterion of 1.5 to 2 mm may improve accuracy and better reconcile the differences between observed and simulated wet day patterns compared to using a 1 mm threshold. However, the ensemble model for the MAM season in the East Africa region underestimates various precipitation statistics, including the amount of precipitation on wet days (PRCPTOT), the frequency of extremely wet days (R95p), the intensity of precipitation on wet days (SDII), and the number of heavy precipitation days (R20mm). On the other hand, the findings from [22] show that the model overestimates the duration of consecutive dry days.

## 3.2 Projected changes in wet days and dry spells patterns in individual CMIP6 models

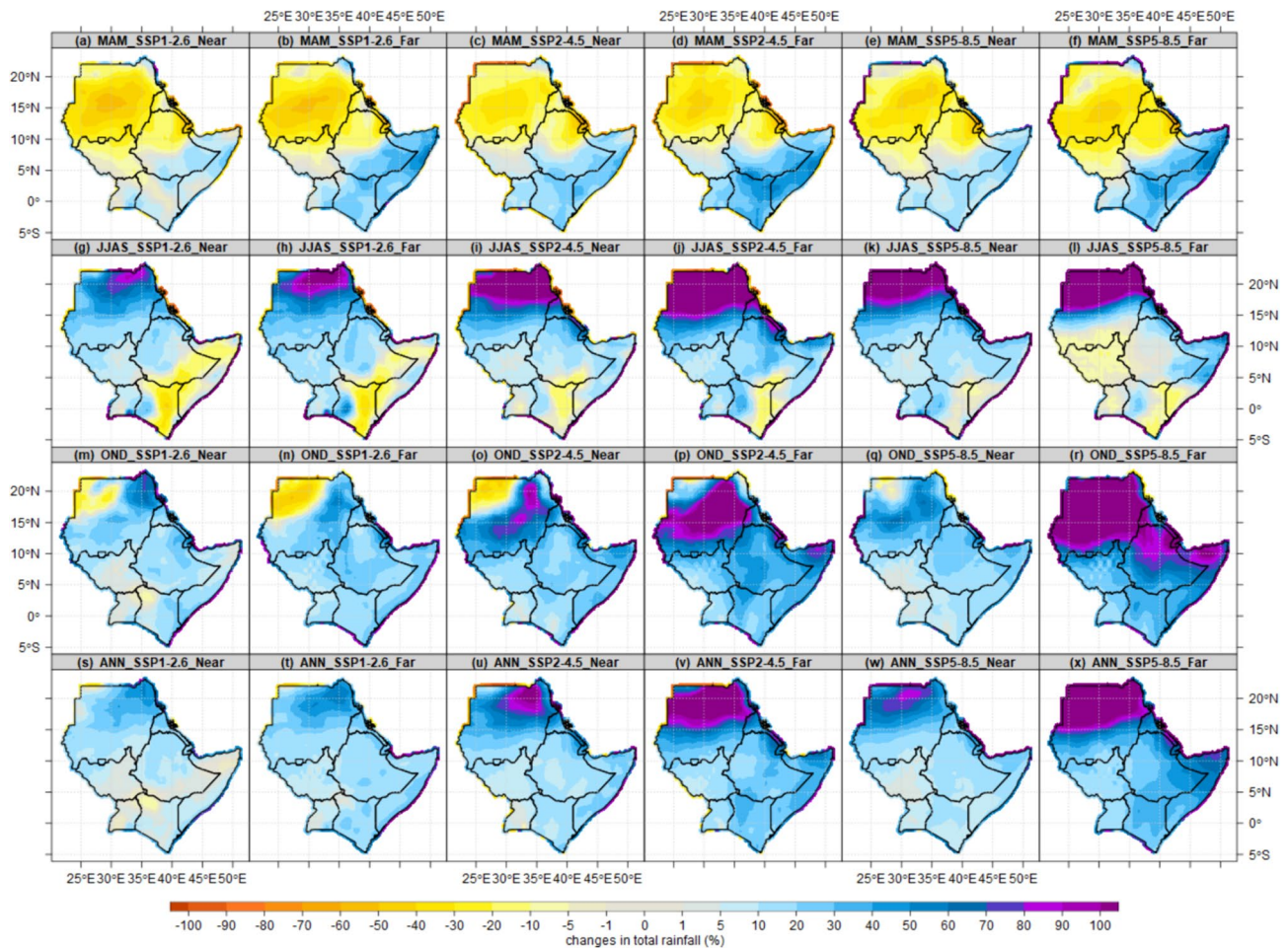
### 3.2.1 Projected changes in total rainfall and intensity

Figure 5 illustrates the spatial distribution of projected total rainfall across the IGAD region. The analysis considers two future periods: the near future (2021–2050) and the far future (2071–2100), compared to a baseline period (1985–2014). We examined three emission scenarios (SSP1-2.6, SSP2-4.5, and SSP5-8.5) for four seasons: MAM (top row), JJAS (second row), OND (third row), and Annual (ANN) in the bottom row. The first, third, and fifth columns display the near future, while the second, fourth, and sixth columns represent the far future. The findings indicate a projected decrease in total rainfall during the MAM season for the entire country of Sudan, as well as the northern and central parts of South Sudan and Ethiopia. On the other hand, western Kenya, Somalia, and Uganda are forecasted to experience an overall increase in rainfall across all seasons and scenarios throughout MAM (Fig. 5a–f). The JJAS season is expected to have a longer dry period in the ASALs of Kenya and southern Somalia, as well as in Sudan, South Sudan, Ethiopia, northern Somalia, and the western and Nyanza regions of Kenya (Fig. 5g–l). During the OND season, all three scenarios show an increase in total rainfall across the IGAD region, except for the northwestern



**Fig. 4** Annual cycle of simulated number of wet days over El Gadaref (Sudan), the Upper Nile (South Sudan), Arsi (Ethiopia), Trans Nzoia (Kenya), and Arua (Uganda). The analysis based on 10 bests performed CMIP6 models and EnsMean in black, CHIRPS v2.0 reference datasets(red) and 1985–2014 baseline

areas of Sudan (Fig. 5m–r). Overall, the region is projected to experience an increase in total annual rainfall in both the near future (2021–2050) and the far future (2071–2100). The projected increase in rainfall patterns by end of century in agreement with study by [60], contrary to the study by [61] over East and Northern Africa, which projected a decrease in precipitation of up to 133 mm over North and East Africa. In the next subsections, the role played by changes in daily rainfall intensity, wet/dry days, and wet/dry spells in the increase/decrease in annual and seasonal projections presented.



**Fig. 5** Spatial pattern of projected changes (%) in total rainfall over the IGAD region based on CMIP6 EnsMean for the near future (2021–2050) and far future (2071–2100) relative to the baseline period (1985–2014). The near future presented in (first, third and fifth columns) and far future (second, fourth and sixth columns). The MAM season presented in (first row), JJAS (second row), OND (third row) and Annual (fourth row)

### 3.3 Projected changes in rainfall intensity

It is evident that changes in rainfall intensity directly correspond to changes in total rainfall patterns, as explained in the previous section (Fig. 5). The rainfall intensity (Fig. 6) indicates a decrease in rainfall intensity across all emission scenarios during the MAM season in Sudan, the central and northern parts of South Sudan, and Ethiopia. Similarly, Western Kenya, Somalia, and Uganda are projected to experience a decrease in rainfall intensity across all seasons and scenarios (SSP1-2.6, SSP2-4.5, SSP5-8.5) during MAM (Fig. 6a–f). Additionally, just like the total rainfall, the JJAS season is projected to have an increase in rainfall intensity over Sudan, South Sudan, Ethiopia, northern Somalia, and western Nyanza provinces in Kenya (Fig. 6g–l). On the other hand, the dry season in the ASALs of Kenya and southwestern Somalia is expected to see an increase. With the exception of the north-western parts of Sudan, the rainfall intensity for the OND season and annual patterns (Fig. 6m–r, s–x) is projected to increase in the region across all three scenarios in the near future (2021–2050) and the far future (2071–2100), which partly in agreement with studies by [32, 62], and [61].

### 3.4 Projected changes in wet days and wet spells patterns

The projected number of wet days across the IGAD region shows that southern and central Uganda recorded the highest number of wet days (60–80 days) during the MAM season under the SSP1-2.6, SSP2-4.5, and SSP5-8.5 scenarios at the 1 mm threshold (Fig. 7a–f). The highlands of western Ethiopia are projected to experience more than

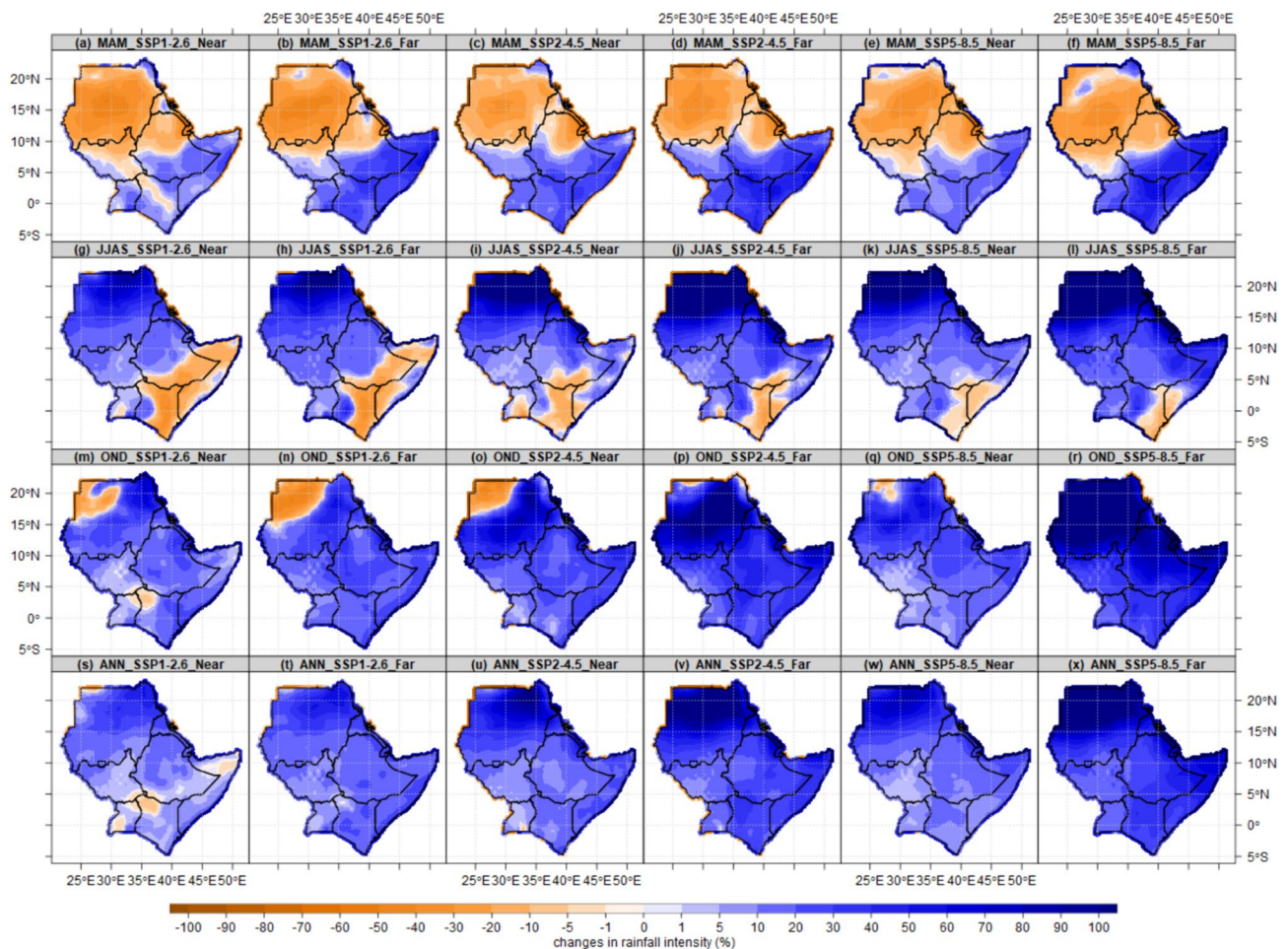


**Fig. 6** The spatial distribution of projected rainfall intensity across the IGAD area for the near future (2021–2050) and far future (2071–2100) based on CMIP6 EnsMean compared to the baseline period (1985–2014). The near future presented in (first, third and fifth columns) and far future (second, fourth and sixth columns). The MAM season presented in (first row), JJAS (second row), OND (third row) and Annual (fourth row)

110–120 days out of a possible 122 wet days, followed by the majority of parts of South Sudan, northern Uganda, and western Kenya (90–110 days) during the JJAS season under all three scenarios (Fig. 7g–l). Coastal and southern parts of Kenya, southern and central Uganda, and southwestern Ethiopia are projected to experience the highest number of wet days (60–80 days) out of the 92 possible days during the OND season under all three scenarios (Fig. 7m–r). The regions with the highest and lowest number of wet and dry days are consistent with the findings of [47], particularly in Equatorial Eastern Africa. The highest number of wet days projected annually is over Uganda, South Sudan, and the highlands of western Ethiopia, while the lowest number of wet days is projected over central and northern Sudan, Djibouti, Eritrea, and northern Somalia (Fig. 7s–x). The areas with the highest and lowest number of wet days are the same regions projected to have high exposure to extreme rainfall events over East Africa [32]. During the DJF, MAM, and OND dry seasons, most parts of Sudan and Kenya are projected to experience the lowest number of wet days (0–20 days) out of 91, 122, and 92 days, respectively. Only the desert and semi-desert in the northern parts of Sudan are projected to experience less than 10 days across all seasons and scenarios. This desert spans an average of 63–179 km in central and northern Sudan [63]. The highest number of wet days over the highlands of western Ethiopia, most parts of Uganda and South Sudan, and western Kenya indicates a high probability of a conducive environment for rain-fed agriculture and food security. The arid and semi-arid regions in northern and northeastern Kenya, northern Sudan, most parts of Somalia, Djibouti, and Eritrea have a high chance of consecutive dry conditions, recurrent water scarcity situations, and food insecurity. In general, there is an overestimation of wet days by CMIP6 at the 1 mm threshold when comparing the projected number of wet days under all scenarios with the CHIRPs reference dataset presented in Fig. 2B, C.

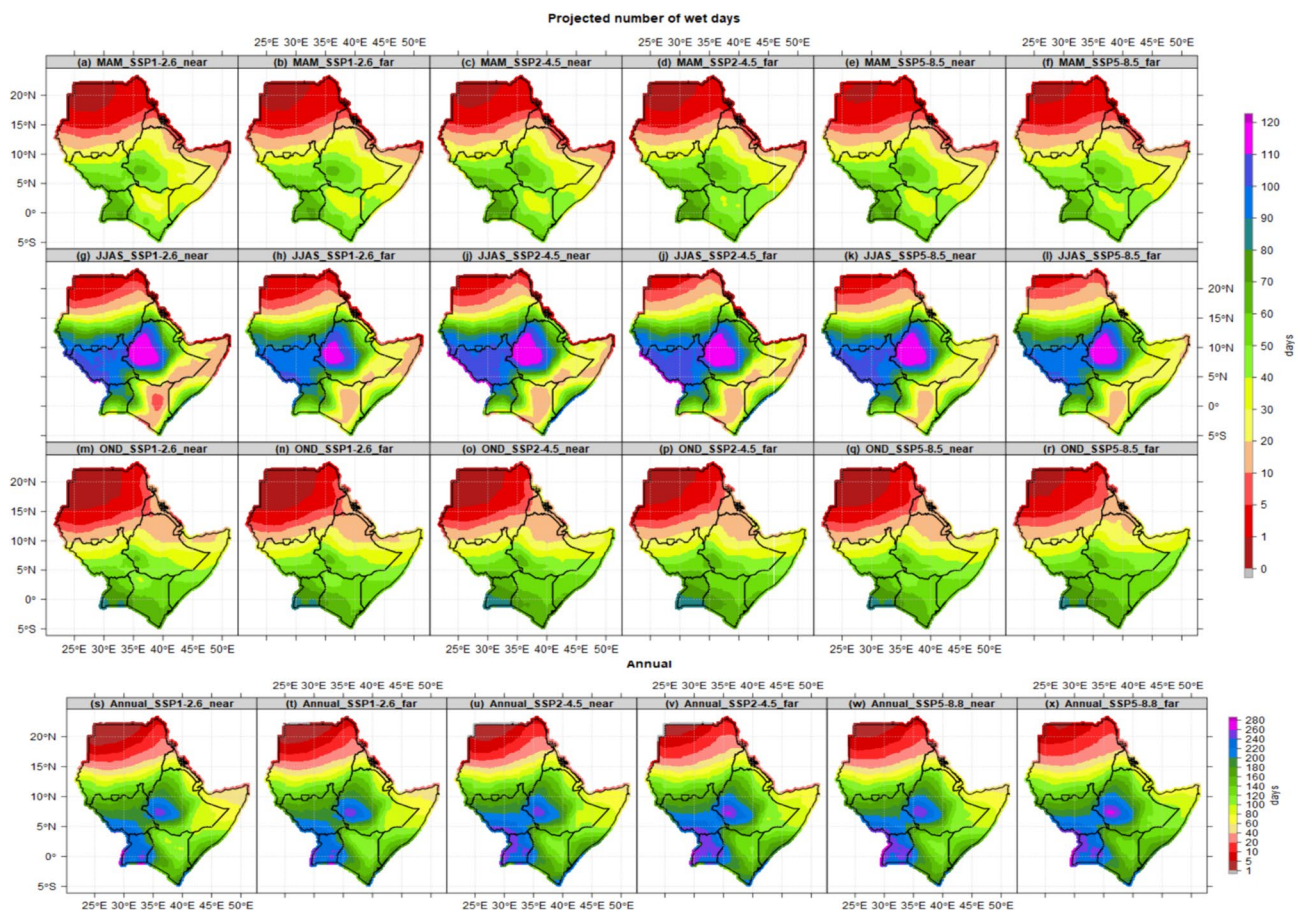


**Fig. 7** The spatial distribution of projected changes in wet days occurrences over the IGAD region for the near future (2021–2050) and far future (2071–2100) compared to the reference period (1985–2014). The near future presented in (first, third and fifth columns) and far future (second, fourth and sixth columns). The MAM season presented in (first row), JJAS (second row), OND (third row) and Annual (fourth row)

The spatial patterns of wet spells are projected to change in different countries in the IGAD region. Under all scenarios and in the near and far future, it is projected that there will be fewer consecutive wet spells during the annual and MAM seasons in Sudan, South Sudan, northern Uganda, western and northern Ethiopia, Eritrea, and Djibouti (Fig. 8). However, the central and northern parts of Sudan are projected to experience an increase in wet spells due to an increase in the number of wet days during the JJAS, OND, and annual periods as reported in a study by [34]. In the southern and central parts of South Sudan, the main rainy season of JJAS is projected to decrease, which will have significant impacts on rain-fed agriculture. On a more positive note, Nyanza and western counties in Kenya, which are considered potential agricultural areas, are projected to receive more wet spells. This will create more favorable conditions for agriculture, food and cash crops productivity. Furthermore, an increase in wet spells, along with the projected increase in total rainfall patterns reported in Sect. 3.2, could lead to a decrease in the frequency and intensity of drought over most parts of East Africa in the far future (2071–2100) under SSP1-2.6, SSP2-4.5, and SSP5-8.5, as indicated in the study by [64]. Other studies, such as [20], have also shown an increase in wet days and spells in CMIP6 models, as well as projected increases in extreme temperature patterns and the association between extreme rainfall events and the frequency and severity of drought patterns in East Africa [54, 65].

Figures 9 and 10 illustrate the temporal patterns of wet days and uncertainty in CMIP6 GCMs across five different food baskets in the IGAD region. The number of wet days is projected to increase during the MAM season in Upper Nile state, located in the northeastern part of South Sudan, Arsi zone in the center of Ethiopia, and Trans Nzoia county in western Kenya. Conversely, there will be a decrease in the number of wet days for SSP5-8.5 scenarios during the JJAS season. The results indicate that by the end of the century, the changes in wet days (increase/decrease) will be more significant for SSP5-8.5 emission scenarios compared to SSP1-2.6 emission scenarios. Notably, the magnitude of these changes is

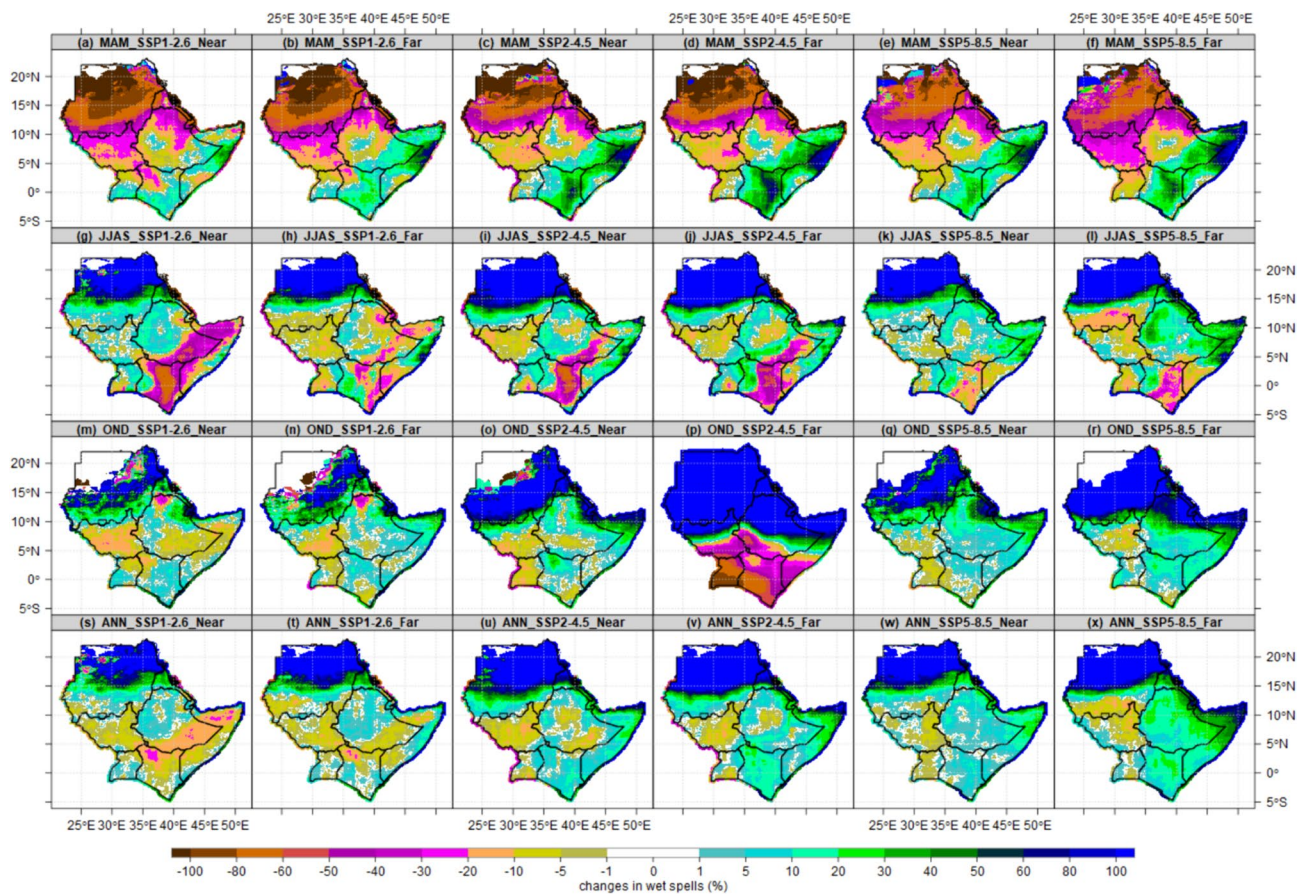
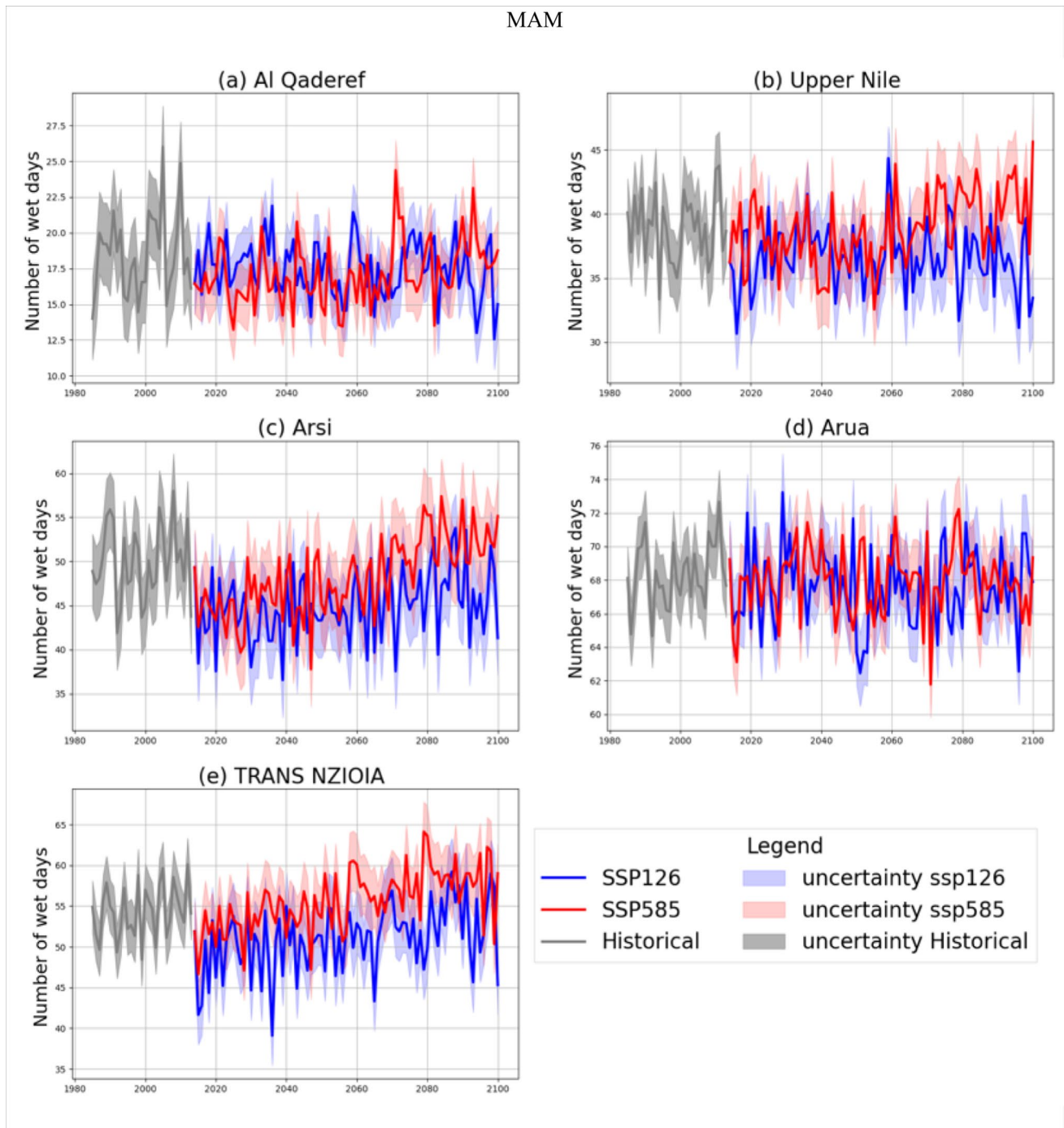


**Fig. 8** The spatial distribution of projected changes(%) in wet spells occurrences over the IGAD region for the near future (2021–2050) and far future (2071–2100) compared to the baseline period (1985–2014). The near future presented in (first, third and fifth columns) and far future (second, fourth and sixth columns). The MAM season presented in (first row), JJAS (second row), OND (third row) and Annual (fourth row)

higher over Al Qadaref and Upper Nile. These findings suggest that if we continue with business as usual (less sustainable climate policies), there will be more wet days (and prolonged dry spells) in various parts of the IGAD in the future. The severity of the dry season (MAM) and wet season (JJAS) in Sudan will increase, while South Sudan will experience a decrease in the wet season during JJAS and OND seasons.

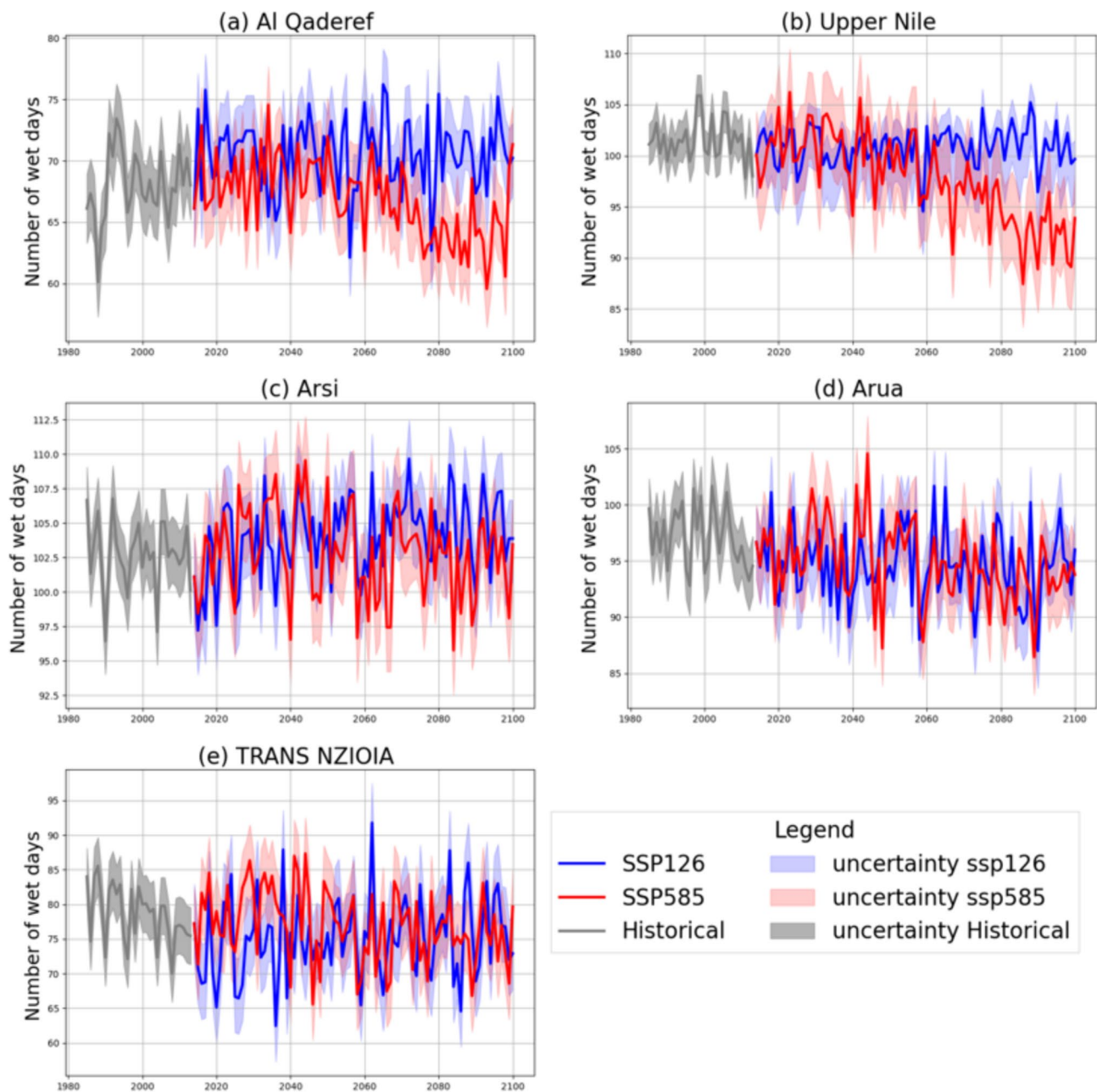
The uncertainty in SSP1-2.6 and SSP5-8.5, as identified by 10 models, highlights the epistemic uncertainties in simulation and projections due to a lack of knowledge or information about a system, process, or phenomenon, as well as internal variations in model outputs resulting from the inherent dynamics and complexity of the modeled system [66]. It is crucial to consider the ensemble mean rather than individual models. This highlights the need to quantify uncertainty in CMIP6 GCMs, as there is no consensus among models regarding the future changes in rainfall [67]. Furthermore, when comparing the near future (2021–2050) to the far future (2071–2100), the level of uncertainty increases, particularly under the SSP585 scenario. The convective parameterization scheme in GCMs has been identified as the main source of this uncertainty [68].

The boxplots in Fig. 11 demonstrate the median (represented by a thick horizontal line) of wet day anomalies for the low SSP1-2.6 and SSP5-8.5 scenarios in five locations within the IGAD region. Interestingly, the median for the low emissions scenario is below 0, while the median for the high emissions scenario is above 0. This suggests that there is a higher climate sensitivity in CMIP6, which aligns with previous findings in other CMIP versions [20]. Additionally, the boxplots and whiskers also indicate that the variations in wet day patterns are more pronounced during the OND season compared to the MAM and JJAS seasons. These changes are likely influenced by projected anomalies in sea surface temperatures (SSTs) and episodes of the El Niño–Southern Oscillation (ENSO), which significantly affect East Africa during the OND season [69].



**Fig. 9** The projected temporal patterns of uncertainty in wet days during MAM season over El Gadaref (Sudan), the Upper Nile(South Sudan), Arsi (Ethiopia),Trans Nzoia ( Kenya), and Arua ( Uganda) for SSP1-2.6 and SSP5-8.5 for the period 1985 to 2100. The blue (red) line shows the EnsMean, blue and brown filled range correspond to the uncertainty bound of the 10-best performed CMIP6 models. The y-axis represents years under analysis from 1981 to 2100 and x-axis represent number of wet days and years

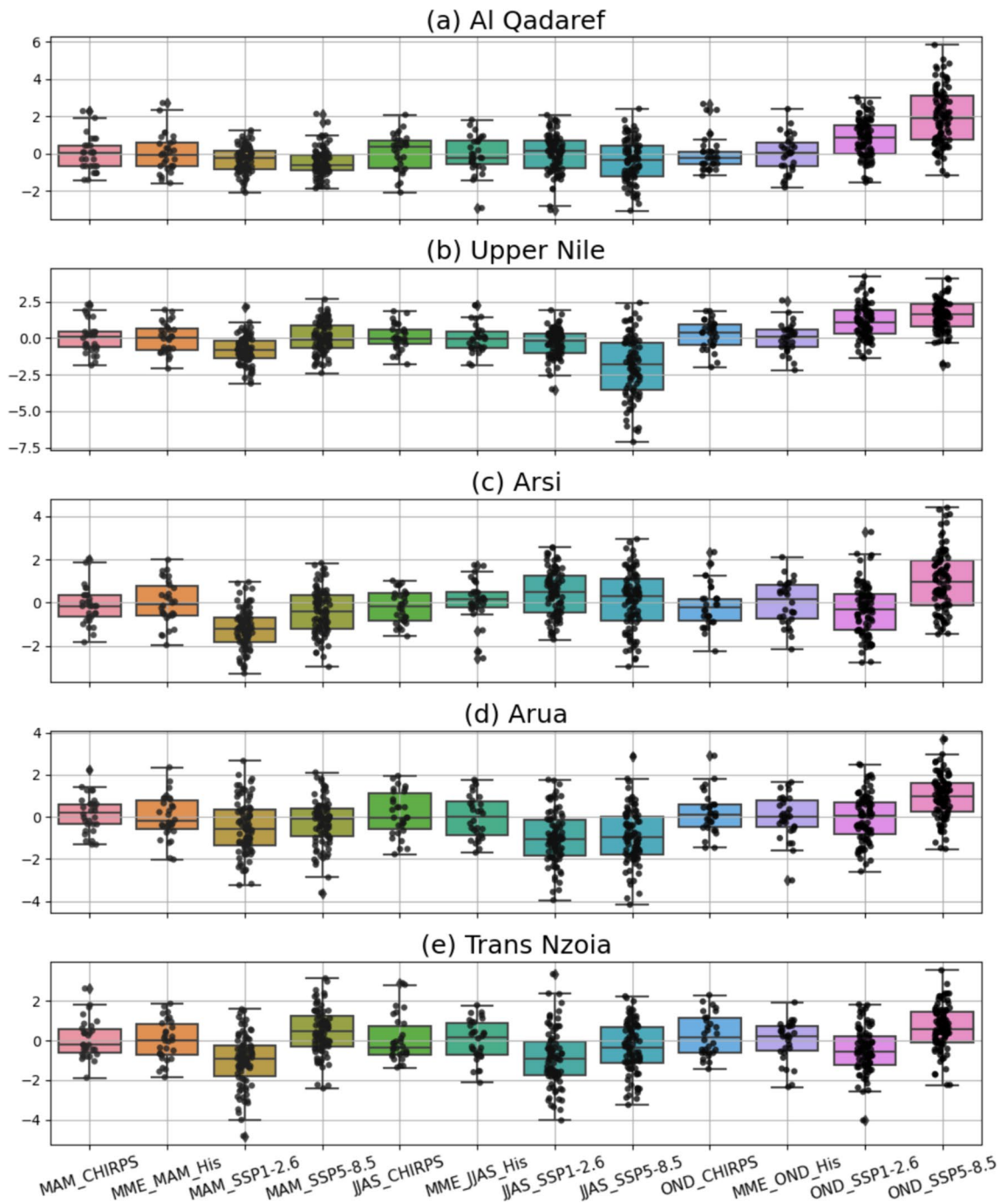
It is worth noting that the most substantial decrease and fluctuation in consecutive wet days are expected to occur during the JJAS season under both SSP1-2.6 and SSP5-8.5 scenarios. This finding is consistent with the research of [70] and [21], which highlight that the most significant reductions in consecutive wet days in East Africa are observed at GW levels of 1.5 °C and 2 °C.



**Fig. 10** The projected temporal patterns of uncertainty in wet days during JJAS season over El Gadaref (Sudan), the Upper Nile (South Sudan), Arsi (Ethiopia), Trans Nzoia (Kenya), and Arua (Uganda) for SSP1-2.6 and SSP5-8.5 for the period 1985–2100. The blue (red) line shows the EnsMean, blue and brown filled range correspond to the uncertainty bound of the 10-best performed CMIP6 models. The y-axis represents years under analysis from 1981 to 2100 and x-axis represent number of wet days and years

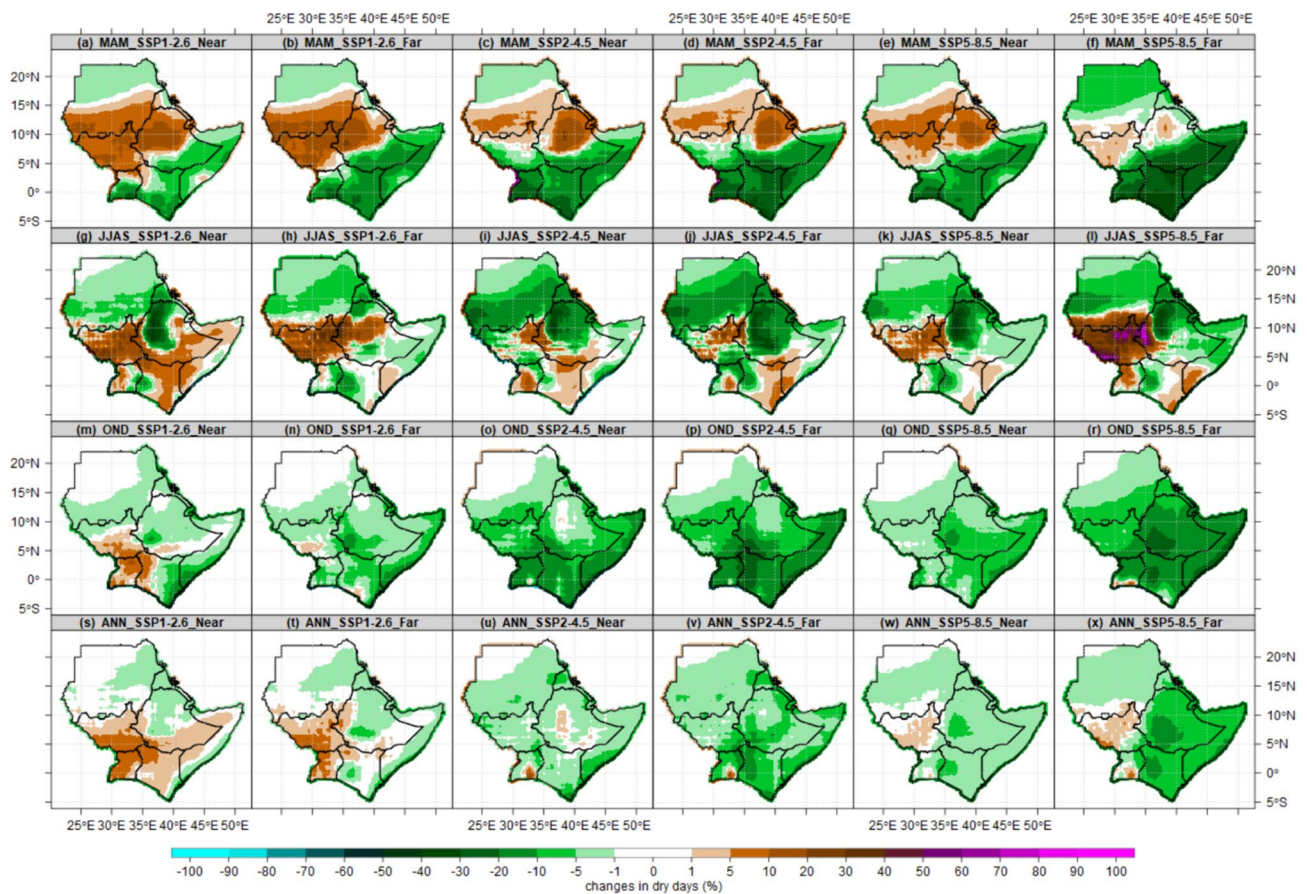
### 3.5 Projected changes in dry spells patterns

Figure 12 shows the spatial distribution of projected changes in the frequency of dry days in the IGAD region for the seasons MAM, JJAS, OND, and annually, considering three different emission scenarios. The EnsMean patterns reveal a significant and widespread decrease in the frequency of dry days in the future across all three seasons and scenarios. Projections suggest that countries such as Kenya, Uganda, Somalia, and southeastern Ethiopia will experience a reduction of between 5 and 15 percent in the total number of dry days during the MAM season. The desert and semi-arid regions in northern Sudan are also expected to see a decrease of 1–10% in dry days, indicating a decrease in the intensity of



**Fig. 11** The Boxplots show standardized anomalies of wet days over El Gadaref (Sudan), the Upper Nile (South Sudan), Arsi (Ethiopia), Trans Nzoia (Kenya), and Arua (Uganda) for SSP1-2.6 and SSP5-8.5 for the period 1985–2100

desert-like conditions in the future across all seasons. According to the SSP1-2.6 scenario, the rain belt region in Sudan, western and northern Ethiopia, and most parts of South Sudan are projected to experience an increase in dry days, particularly during MAM, in both the near and distant future. The OND season is expected to see an increase in the number of dry days throughout the entire IGAD region. These trends contradict the observed increase in the maximum number of continuous dry days (CDD) in the CORDEX-Africa experiment and the occurrence of drought in CMIP5 [71] in East Africa. Furthermore, the study conducted by [72] confirms increased rainfall in the highlands of Ethiopia, which aligns with the main driver identified by Gebrechorkos et al. (2023) for the projected rise in total precipitation across East Africa as projected by the CMIP6 model.



**Fig. 12** The spatial distribution of projected changes (%) in dry days occurrences over the IGAD region for the near future (2021–2050) and far future (2071–2100) compared to the reference period (1985–2014). The near future presented in (first, third and fifth columns) and far future (second, fourth and sixth columns). The MAM season presented in (first row), JJAS (second row), OND (third row) and Annual (fourth row)

### 3.6 Impacts of ensemble averaging of 10 CMIP6 models outputs

Ensemble averaging of CMIP6 outputs significantly enhances the reliability and usefulness of climate projections by reducing individual model biases, improving uncertainty quantification, and providing more robust regional climate projections (Lei et al. 2023). However, it may smooth out some extreme events and face challenges in fully representing model diversity (Jiang An and Yin 2024). Figure 13 presents the projected changes in the number of wet days during the JJAS season under SSP5-8.5 scenarios as a sample of results from total rainfall, rainfall intensity, dry days, wet spells, and dry spells. This was done to assess the inconsistencies between the 10 individual CMIP6 models used to compute the EnsMean and how wet and dry biases have been affected or hidden by the EnsMean. Although the 10 CMIP6 models selected to compute EnsMean are the best performers over the IGAD region, it is clear that there are significant inconsistencies between individual CMIP6 models and the ensemble mean. The EnsMean smooths out extremes (wet and dry) and provides a more general picture of changes in rainfall patterns. Some models have biases toward dry conditions, while others project wet biases. This happens because each CMIP6 model has its own representation of physical processes like convection, cloud formation, and land–atmosphere interactions. The GFDL-ESM4 model projects dry conditions over most parts of the IGAD region. Seven out of ten models (CMCC-CM2-HR4, EC-Earth3, HadGEM3-GC31-MM, INM-CM5-0, IPSL-CM6A-LR, MIROC6, and TaiESM1) project a 60–90% increase in total rainfall, rainfall intensity, wet days, and wet spells over central and northern Sudan during both the near future (2021–2050) and the far future (2071–2100). The dry season of JJAS over eastern and northeastern Kenya and southern parts of Somalia is projected to intensify based on five models (BCC-CSM2-MR, EC-Earth3, GFDL, IPSL-CM6A-LR, and NorESM2-MM) during both the near and far future. The projected decrease in total rainfall, wet days, and wet spells over South Sudan in the far future is driven mostly by

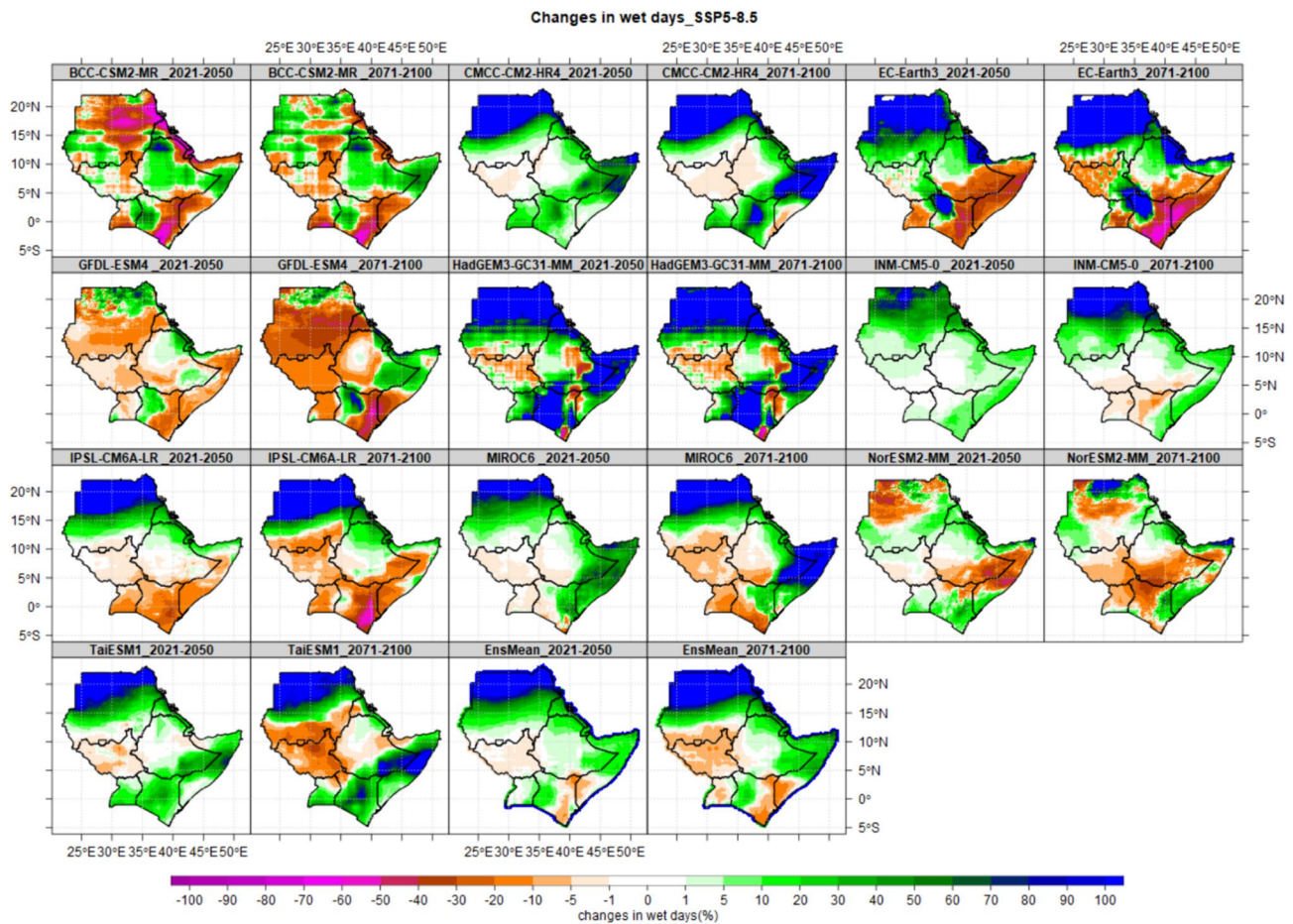


**Fig. 13** The spatial distribution of projected changes (%) in wet day occurrences over the IGAD region for the near future (2021–2050) and far future (2071–2100) compared to the reference period (1985–2014). The analysis for the JJAS season is based on 10 CMIP6 individual Models under SSP5-8.5 scenario

the BCC-CSM2-MR, CMCC-CM2-HR4, EC-Earth3, GFDL-ESM4, NorESM2-MM, and TaiESM1 models. From the analysis of individual CMIP6 models and the EnsMean, it is clear that the impact of EnsMean averaging is significant. The EnsMean tends to smooth out the extremes (wet or dry biases), creating a result that may appear more accurate but does not reflect the extremes or variations projected by individual models. Some CMIP6 models exhibit a dry bias due to underestimating convection or misrepresenting cloud formation, leading to less rainfall in certain regions. Conversely, models with a wet bias may overestimate moisture availability or storm frequency, resulting in higher-than-expected precipitation (Jiang et al. 2024). This occurs because each climate model has its own representation of physical processes like convection, cloud formation, and land–atmosphere interactions (Duan et al. 2021).

#### 4 Conclusions

This study utilized a 23-member CMIP6 and an MME or EnsMean composed of the top-performing 10 CMIP6 models in the IGAD region. The objective was to investigate projected changes in number of wet/dry days and wet/dry spells on an annual and seasonal basis. An analysis was conducted on projected changes for the near future (2021–2050) and far future (2071–2100) compared to the reference period (1985–2014) using three emission scenarios (SSP1-2.6, SSP2-4.5, and SSP5-8.5). When comparing the average number of wet/dry days and wet/dry spells in the CHIRPS v2.0 reference data with the CMIP6 model simulations during the baseline period, it is evident that the majority of the models overestimated both wet days and dry spells across the study region. This overestimation is attributed to the implementation of the 1 mm threshold for rainy days set by the ETCCDI. The ETCCDI's threshold leads to an overestimation of both the frequency of wet days (dry days) and the duration of dry spells (wet spells). Therefore, using a rainfall threshold of 1.5

or 2 mm may be more appropriate for analyzing daily rainfall attributes such as wet/dry days and spells, rainfall intensities, onset and cessation dates, and the duration of the growing season. The CMIP6 ensemble provides a more accurate representation of wet days and dry spells compared to individual models. This finding aligns with the conclusions of [73] and [74], who observed that ensemble means effectively reduce spatial uncertainty and inconsistency by reducing inter-model biases. A projected 10–20% increase in total rainfall over the IGAD region is driven by an increase in rainfall intensity and the number of wet days under all scenarios (SSP1-2.6, SSP2-4.5, SSP5-8.5) during the near (2021–2050) and far (2071–2100) future. In addition, the majority of the IGAD region, there has been a 20–30% increase in wet days and a corresponding 10–20% decrease in the duration of maximum dry spells. Under the SSP5-8.5 scenario, there is an overall decrease in the number of wet days during JJAS, while there is an overall increase in the anomalies of wet days during OND. Furthermore, the results indicate an increase in deviations from the average number of rainy days by the year 2100. Although the ensemble averaging of 10 CMIP6 outputs seems to increase the robustness of findings and reduce individual model-specific biases, uncertainty, and generate consensus projections, it comes with significant drawbacks. These drawbacks include the underestimation of extremes and the obscuring of the valuable diversity of individual model outputs. Additionally, there is a risk of overconfidence in the results, which can mislead policymakers or stakeholders into believing that the ensemble average represents a higher certainty than is warranted. Despite these limitations, ensemble averaging remains a key tool for climate research, adaptation planning, and policy formulation. The analysis highlights the importance of implementing more effective measures to reduce greenhouse gas emissions in order to limit the global temperature increase to 1.5 °C, as outlined in the Paris Agreement. This is evident from the observed changes in the frequency of rainy days and dry spells, which differ between the SSP1-2.6 and SSP5-8.5 scenarios. Additionally, this study did not examine the microscale and mesoscale processes and drivers, nor did it explore the dynamic mechanisms. Moreover, the majority of models exhibited an overestimation of wet days and dry spells patterns, emphasizing the need for further research to understand the additional factors that contributed to this overestimation.

**Acknowledgements** This work is a component of a doctoral research program at the University of Nairobi, Kenya. It is being conducted within the Faculty of Science & Technology, specifically in the Department of Earth & Climate Sciences. The author would like to express gratitude to the World Climate Research Programme (WCRP) Coupled Model Intercomparison Project (Phase 6) and the organizations from the USA, PCMDI/LLNL (California), France, IPSL, Germany, DKRZ, and UK, CEDA, for their efforts in preserving and providing free access to the CMIP6 data.

**Author contribution** All authors conceived and designed the study. Paulino Omoj. Omay prepared, collected, and analyzed data. Paulino Omoj Omay wrote the original draft under the supervision of Nzioka J. Muthama, Christopher Oludhe, and Josiah M. Kinama. Guleid Artan and Zachary Atheru examined the final text. Previous manuscript versions were reviewed by all authors. The article was reviewed and approved by each author.

**Funding** Through the Intra-ACP Climate Services and Related Applications (ClimSA) support to the IGAD Climate Prediction and Application Center (ICPAC), the Authors wish to acknowledge funds that were granted for the open access publishing of this research.

**Data availability** The secondary datasets produced during the analysis can be obtained upon request. The source of CHIRPS v2.0 (Index of products/CHIRPS-2.0 (ucsb.edu)) and CMIP6 (cmip6—Home | ESGF-CoG (llnl.gov)) datasets are freely available online (open sources).

**Code availability** We utilized Climate Data Operators (CDO) and Climate Data Tool (CDT) statistical packages.

## Declarations

**Ethics approval and consent to participate** I hereby affirm that this particular work of writing is my own unique work and has not been submitted for publication anywhere else. In compliance with the rules of the University of Nairobi, any instances in which I have used the work of other persons or my own work have been appropriately recognized and cited. Authors' permission to participate is obtained.

**Consent for publication** This work is published with the cooperation of all authors.

**Competing interests** The authors declare no competing interests.

**Open Access** This article is licensed under a Creative Commons Attribution-NonCommercial-NoDerivatives 4.0 International License, which permits any non-commercial use, sharing, distribution and reproduction in any medium or format, as long as you give appropriate credit to the original author(s) and the source, provide a link to the Creative Commons licence, and indicate if you modified the licensed material. You do not have permission under this licence to share adapted material derived from this article or parts of it. The images or other third party material in this article are included in the article's Creative Commons licence, unless indicated otherwise in a credit line to the material. If material is not included in the article's Creative Commons licence and your intended use is not permitted by statutory regulation or exceeds the permitted use, you will need to obtain permission directly from the copyright holder. To view a copy of this licence, visit <http://creativecommons.org/licenses/by-nc-nd/4.0/>.

## References

1. Ongoma V, Chena H, Gaoa C. Projected changes in mean rainfall and temperature over east Africa based on CMIP5 models. *Int J Climatol.* 2018;38(3):1375–92. <https://doi.org/10.1002/joc.5252>.
2. IPCC, "Climate Change 2013: The Physical Science Basis, Contribution of Working Group I," *Fifth Assessment Report of the Intergovernmental Panel on Climate Change.* 2013.
3. Dessler A. Introduction to modern climate change. Second Edition. 2019. <https://doi.org/10.1017/9781316156490>.
4. Almazroui M, et al. Projected change in temperature and precipitation over Africa from CMIP6. *Earth Syst Environ.* 2020;4(3):455–75. <https://doi.org/10.1007/s41748-020-00161-x>.
5. Omondi PAO, et al. Changes in temperature and precipitation extremes over the Greater Horn of Africa region from 1961 to 2010. *Int J Climatol.* 2014;34(4):1262–77. <https://doi.org/10.1002/joc.3763>.
6. Makula EK, Zhou B. Coupled Model Intercomparison Project phase 6 evaluation and projection of East African precipitation. *Int J Climatol.* 2022;42(4):2398–412. <https://doi.org/10.1002/joc.7373>.
7. Funk C, Nicholson SE, Landsfeld M, Klotter D, Peterson P, Harrison L. The centennial trends greater horn of Africa precipitation dataset. *Sci Data.* 2015. <https://doi.org/10.1038/sdata.2015.50>.
8. Funk C, Harrison L, Alexander L, Peterson P, Behrangi A, Husak G. Exploring trends in wet-season precipitation and drought indices in wet, humid and dry regions. *Environ Res Lett.* 2019;14(11):115002. <https://doi.org/10.1088/1748-9326/ab4a6c>.
9. Wainwright CM, Finney DL, Kilavi M, Black E, Marsham JH. "Extreme rainfall in East Africa, October 2019–January 2020 and context under future climate change." *Weather.* 2020. <https://doi.org/10.1002/wea.3824>.
10. Mbigi D, Onyango A, Mtewe ZF, Kiprotich P, Xiao Z. CMIP6 simulations of the spatial structure of rainfall variability over East Africa: evaluation and projection. *Int J Climatol.* 2022. <https://doi.org/10.1002/joc.7868>.
11. Omay PO, Christopher O, Atheru Z, Atheru Z. Changes and Variability in rainfall onset, cessation and length of rainy season in the IGAD region of Eastern Africa. *Theor Appl Climatol.* 2022. <https://doi.org/10.1007/s00704-023-04433-0>.
12. Breinl K, Di Baldassarre G, Mazzoleni M, Lun D, Vico G. Extreme dry and wet spells face changes in their duration and timing. *Environ Res Lett.* 2020. <https://doi.org/10.1088/1748-9326/ab7d05>.
13. Ojara MA, Yunsheng L, Babaousmail H, Sempa AK, Ayugi B, Ogwang BA. Evaluation of drought, wet events, and climate variability impacts on maize crop yields in East Africa during 1981–2017. *Int J Plant Prod.* 2022;16(1):41–62. <https://doi.org/10.1007/s42106-021-00178-w>.
14. Fall CMN, Lavaysse C, Drame MS, Panthou G, Gaye AT. Wet and dry spells in Senegal: comparison of detection based on satellite products, reanalysis, and in situ estimates. *Nat Hazards Earth Syst Sci.* 2021;21(3):1051–69. <https://doi.org/10.5194/nhess-21-1051-2021>.
15. A. Salami, A. B. Kamara, and Z. Brixiova, "Smallholder Agriculture in East Africa: Trends, Constraints and Opportunities," *Work. Pap. No.105 African Dev. Bank*, no. April, p. 52, 2010, <https://doi.org/10.1111/j.1467-937X.2007.00447.x>.
16. Camberlin P, Fontaine B, Louvet S, Oettli P, Valimba P. Climate adjustments over Africa accompanying the Indian monsoon onset. *J Clim.* 2010. <https://doi.org/10.1175/2009JCLI3302.1>.
17. Betts RA, et al. Changes in climate extremes, fresh water availability and vulnerability to food insecurity projected at 1.5°C and 2°C global warming with a higher-resolution global climate model. *Philos Trans R Soc A Math Phys Eng Sci.* 2018. <https://doi.org/10.1098/rsta.2016.0452>.
18. Taylor KE, Stouffer RJ, Meehl GA. An overview of CMIP5 and the experiment design. *Bull Am Meteorol Soc.* 2012;93(4):485–98. <https://doi.org/10.1175/BAMS-D-11-00094.1>.
19. Eyring V, et al. Overview of the Coupled model intercomparison project phase 6 (CMIP6) experimental design and organization. *Geosci Model Dev.* 2016;9(5):1937–58. <https://doi.org/10.5194/gmd-9-1937-2016>.
20. Wainwright CM, Black E, Allan RP. Future changes in wet and dry season characteristics in CMIP5 and CMIP6 simulations. *J Hydrometeorol.* 2021. <https://doi.org/10.1175/jhm-d-21-0017.1>.
21. Gudoshava M, et al. Projected effects of 1.5 °C and 2 °C global warming levels on the intra-seasonal rainfall characteristics over the Greater Horn of Africa. *Environ Res Lett.* 2020;15(3):34037. <https://doi.org/10.1088/1748-9326/ab6b33>.
22. Ayugi B, et al. Comparison of CMIP6 and CMIP5 models in simulating mean and extreme precipitation over East Africa. *Int J Climatol.* 2021;41(15):6474–96. <https://doi.org/10.1002/joc.7207>.
23. Dong T, Dong W. Evaluation of extreme precipitation over Asia in CMIP6 models. *Clim Dyn.* 2021;57(7–8):1751–69. <https://doi.org/10.1007/s00382-021-05773-1>.
24. Samantaray AK, Ramadas M, Panda RK. Changes in drought characteristics based on rainfall pattern drought index and the CMIP6 multi-model ensemble. *Agric Water Manag.* 2022;266:107568. <https://doi.org/10.1016/j.agwat.2022.107568>.
25. Brunner L, Lorenz R, Zumwald M, Knutti R. Quantifying uncertainty in European climate projections using combined performance-independence weighting. *Environ Res Lett.* 2019. <https://doi.org/10.1088/1748-9326/ab492f>.
26. Hong J, Javan K, Shin Y, Park JS. Future projections and uncertainty assessment of precipitation extremes in Iran from the cmip6 ensemble. *Atmosphere (Basel).* 2021;12(8):1–16. <https://doi.org/10.3390/ATMOS12081052>.
27. Beobide-Arsuaga G, Bayr T, Reintges A, Latif M. Uncertainty of ENSO-amplitude projections in CMIP5 and CMIP6 models. *Clim Dyn.* 2021;56(11–12):3875–88. <https://doi.org/10.1007/s00382-021-05673-4>.
28. Wainwright CM, Allan RP, Black E. Consistent trends in dry spell length in recent observations and future projections. *Geophys Res Lett.* 2022;49(12):1–15. <https://doi.org/10.1029/2021GL097231>.
29. Dike VN, Lin Z, Fei K, Langendijk GS, Nath D. Evaluation and multimodel projection of seasonal precipitation extremes over central Asia based on CMIP6 simulations. *Int J Climatol.* 2022. <https://doi.org/10.1002/joc.7641>.
30. Adeyeri OE, et al. The trend and spatial spread of multisectoral climate extremes in CMIP6 models. *Sci Rep.* 2022;12(1):1–19. <https://doi.org/10.1038/s41598-022-25265-4>.
31. Lehner F, et al. Partitioning climate projection uncertainty with multiple large ensembles and CMIP5/6. 2020. *Earth Syst Dyn.* <https://doi.org/10.5194/esd-11-491-2020>.

32. Ayugi B, Dike V, Ngoma H, Babaousmail H, Mumo R, Ongoma V. Future changes in precipitation extremes over east Africa based on CMIP6 models. *Water* (Switzerland). 2021. <https://doi.org/10.3390/w13172358>.
33. Ayugi B, et al. Projected changes in meteorological drought over East Africa inferred from bias-adjusted CMIP6 models. *Nat Hazards*. 2022;113(2):1151–76. <https://doi.org/10.1007/s11069-022-05341-8>.
34. Omay PO, Muthama NJ, Oludhe C, Kinama JM, Artan G, Atheru Z. Observed changes in wet days and dry spells over the IGAD region of eastern Africa. *Sci Rep*. 2023;13(1):1–20. <https://doi.org/10.1038/s41598-023-44115-5>.
35. Omay PO, Muthama NJ, Oludhe C, Kinama JM, Artan G, Atheru Z. Evaluation of CMIP6 historical simulations over IGAD region of Eastern Africa. *Discov Environ*. 2023. <https://doi.org/10.1007/s44274-023-00012-2>.
36. Funk CC, et al. A quasi-global precipitation time series for drought monitoring. *U S Geol Surv Data Ser*. 2014;832:4. <https://doi.org/10.3133/ds832>.
37. Kimani MW, Hoedjes JCB, Su Z. An assessment of satellite-derived rainfall products relative to ground observations over East Africa. *Remote Sens*. 2017. <https://doi.org/10.3390/rs9050430>.
38. Cattani E, Merino A, Levizzani V. Evaluation of monthly satellite-derived precipitation products over East Africa. *J Hydrometeorol*. 2016. <https://doi.org/10.1175/JHM-D-15-0042.1>.
39. Dinku T, et al. Validation of the CHIRPS satellite rainfall estimates over eastern Africa. *Q J R Meteorol Soc*. 2018. <https://doi.org/10.1002/qj.3244>.
40. Gebrechorkos SH, Hülsmann S, Bernhofer C. Evaluation of multiple climate data sources for managing environmental resources in East Africa. 2018. *Hydrol Earth Syst Sci*. <https://doi.org/10.5194/hess-22-4547-2018>.
41. Ayugi B, Tan G, Ullah W, Boiyo R, Ongoma V. Inter-comparison of remotely sensed precipitation datasets over Kenya during 1998–2016. *Atmos Res*. 2019;225:96–109. <https://doi.org/10.1016/j.atmosres.2019.03.032>.
42. Dinku T, et al. Validation of the CHIRPS satellite rainfall estimates over eastern Africa. *Q J R Meteorol Soc*. 2018;144(August):292–312. <https://doi.org/10.1002/qj.3244>.
43. Ocen E, de Bie CAJM, Onyutha C. Investigating false start of the main growing season: a case of Uganda in East Africa. *Heliyon*. 2021;7(11):e08428. <https://doi.org/10.1016/j.heliyon.2021.e08428>.
44. Kirkland EJ. “Bilinear interpolation”, in advanced computing in electron microscopy. Boston: Springer; 2010.
45. Fall CMN, Lavaysse C, Drame MS, Panthou G, Gaye AT. Wet and dry spells in Senegal: evaluation of satellite-based and model re-analysis rainfall estimates. 2019. *Nat Hazards Earth Syst Sci Discuss*. <https://doi.org/10.5194/nhess-2019-185>.
46. Goddard L, Gershunov A. Impact of El Niño on weather and climate extremes. *Geophys Monogr Ser*. 2020;253(72):361–75. <https://doi.org/10.1002/9781119548164.ch16>.
47. Gitau W, Ogallo L, Camberlin P, Okoola R. Spatial coherence and potential predictability assessment of intraseasonal statistics of wet and dry spells over Equatorial Eastern Africa. *Int J Climatol*. 2013;33(12):2690–705. <https://doi.org/10.1002/joc.3620>.
48. Seneviratne SI, et al. “Changes in climate extremes and their impacts on the natural physical environment.” *Manag Risks Extrem Events Disasters to Adv Clim Chang Adapt Spec Rep Intergov Panel Clim Chang*. 2012;9781107025:109–230. <https://doi.org/10.1017/CBO9781139177245.006>.
49. Polade SD, Pierce DW, Cayan DR, Gershunov A, Dettinger MD. The key role of dry days in changing regional climate and precipitation regimes. *Sci Rep*. 2014;4:1–8. <https://doi.org/10.1038/srep04364>.
50. Giorgi F, Raffaele F, Coppola E. The response of precipitation characteristics to global warming from climate projections. *Earth Syst Dyn*. 2019;10(1):73–89. <https://doi.org/10.5194/esd-10-73-2019>.
51. Ayugi B, et al. East African population exposure to precipitation extremes under 1.5 °C and 2.0 °C warming levels based on CMIP6 models. *Environ Res Lett*. 2022;17(4):44051. <https://doi.org/10.1088/1748-9326/ac5d9d>.
52. Zarrin A, Dadashi-Roudbari AA. Projected consecutive dry and wet days in Iran based on CMIP6 bias-corrected multi-model ensemble. *J Earth Sp Phys*. 2021;47(3):561–578. <https://doi.org/10.22059/JESPHYS.2021.319270.1007295>.
53. Kim YH, Min SK, Zhang X, Sillmann J, Sandstad M. Evaluation of the CMIP6 multi-model ensemble for climate extreme indices. *Weather Clim Extrem*. 2020;29:100269. <https://doi.org/10.1016/j.wace.2020.100269>.
54. Babaousmail H, et al. Projection of the diurnal temperature range over Africa based on CMIP6 simulations. *J African Earth Sci*. 2023;200:104883. <https://doi.org/10.1016/j.jafrearsci.2023.104883>.
55. Dinku T, et al. ENACTS: advancing climate services across Africa. *Front Clim*. 2022;3(January):1–16. <https://doi.org/10.3389/fclim.2021.787683>.
56. Akinsanola AA, Ongoma V, Kooperman GJ. Evaluation of CMIP6 models in simulating the statistics of extreme precipitation over Eastern Africa. *Atmos Res*. 2021;254:105509. <https://doi.org/10.1016/j.atmosres.2021.105509>.
57. Endris HS, Lennard C, Hewitson B, Dosio A, Nikulin G, Panitz HJ. Teleconnection responses in multi-GCM driven CORDEX RCMs over Eastern Africa. *Clim Dyn*. 2016;46(9–10):2821–46. <https://doi.org/10.1007/s00382-015-2734-7>.
58. Nicholson SE. Climate and climatic variability of rainfall over eastern Africa. *Rev Geophys*. 2017;55(3):590–635. <https://doi.org/10.1002/2016RG000544>.
59. Mbigi D, Onyango AO, Mtewe ZF, Kiprotich P, Xiao Z. Coupled model intercomparison project phase 6 simulations of the spatial structure of rainfall variability over East Africa: evaluation and projection. *Int J Climatol*. 2022;42(16):9865–85. <https://doi.org/10.1002/joc.7868>.
60. Gebrechorkos SH, Taye MT, Birhanu B, Solomon D, Demissie T. Future changes in climate and hydroclimate extremes in East Africa. *Earth's Futur*. 2023;11(2):1–21. <https://doi.org/10.1029/2022EF003011>.
61. Majdi F, Hosseini SA, Karbalaee A, Kaseri M, Marjanian S. Future projection of precipitation and temperature changes in the Middle East and North Africa (MENA) region based on CMIP6. *Theor Appl Climatol*. 2022;147(3):1249–62. <https://doi.org/10.1007/s00704-021-03916-2>.
62. Dosio A, et al. Projected future daily characteristics of African precipitation based on global (CMIP5, CMIP6) and regional (CORDEX, CORDEX-CORE) climate models. *Clim Dyn*. 2021;57(11–12):3135–58. <https://doi.org/10.1007/s00382-021-05859-w>.
63. Mohamed NAH, Osman HMF, El Deen SZ. Rainfall changes in central Sudan between 1960–2010 rainfall changes in central Sudan. *Int J Geosci Geomatics*. 2014;2(1):61–7.
64. Uwimbabazi J, Jing Y, Iyakaremye V, Ullah I, Ayugi B. Observed changes in meteorological drought events during 1981–2020 over Rwanda, East Africa. *Sustain*. 2022. <https://doi.org/10.3390/su14031519>.

65. Das P, et al. Historical and projected changes in Extreme High Temperature events over East Africa and associated with meteorological conditions using CMIP6 models. *Glob Planet Change*. 2023;222:104068. <https://doi.org/10.1016/j.gloplacha.2023.104068>.
66. Adeyeri OE, Zhou W, Ndehedehe CE, Wang X, Ishola KA, Laux P. Minimizing uncertainties in climate projections and water budget reveals the vulnerability of freshwater to climate change. *One Earth*. 2024;7(1):72–87. <https://doi.org/10.1016/j.oneear.2023.12.013>.
67. Choi YW, Campbell DJ, Eltahir EAB. Near-term regional climate change in East Africa. *Clim Dyn*. 2022. <https://doi.org/10.1007/s00382-022-06591-9>.
68. Zhang GJ, McFarlane NA. Sensitivity of climate simulations to the parameterization of cumulus convection in the canadian climate centre general circulation model. *Atmos Ocean*. 1995;33(3):407–46. <https://doi.org/10.1080/07055900.1995.9649539>.
69. Endris HS, Lennard C, Hewitson B, Dosio A, Nikulin G, Artan GA. Future changes in rainfall associated with ENSO, IOD and changes in the mean state over Eastern Africa. *Clim Dyn*. 2019;52(3–4):2029–53. <https://doi.org/10.1007/s00382-018-4239-7>.
70. Osima S, et al. Projected climate over the Greater Horn of Africa under 1.5 °c and 2 °c global warming. *Environ Res Lett*. 2018. <https://doi.org/10.1088/1748-9326/aaba1b>.
71. Haile GG, et al. Projected impacts of climate change on drought patterns over East Africa. *Earth's Futur*. 2020. <https://doi.org/10.1029/2020EF001502>.
72. Tegegne G, Melesse AM, Alamirew T. Projected changes in extreme precipitation indices from CORDEX simulations over Ethiopia, East Africa. *Atmos Res*. 2021;247:105156. <https://doi.org/10.1016/j.atmosres.2020.105156>.
73. Milinski S, Maher N, Olonscheck D. How large does a large ensemble need to be? *Earth Syst Dyn*. 2020;11(4):885–901. <https://doi.org/10.5194/esd-11-885-2020>.
74. Sian KTCLK, Wang J, Ayugi BO, Nooni IK, Ongoma V. Multi-decadal variability and future changes in precipitation over Southern Africa. *Atmosphere (Basel)*. 2021. <https://doi.org/10.3390/atmos12060742>.

**Publisher's Note** Springer Nature remains neutral with regard to jurisdictional claims in published maps and institutional affiliations.